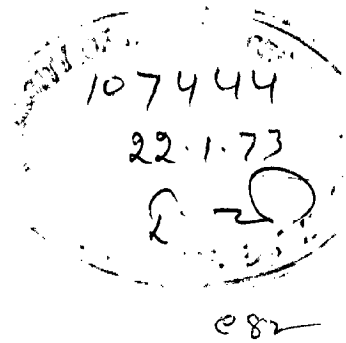


✓  
PH 11-12  
KUM

# STUDY OF KINETICS OF ROASTING OF ZINC SULPHIDE

A DISSERTATION  
submitted in partial fulfilment of the  
requirements for the award of the degree  
of  
MASTER OF ENGINEERING  
in  
METALLURGICAL ENGINEERING  
(EXTRACTIVE METALLURGY)

By  
**SURENDRA KUMAR**



DEPARTMENT OF METALLURGICAL ENGINEERING  
UNIVERSITY OF ROORKEE  
ROORKEE (INDIA)  
August, 1972

IP

C E R T I F I C A T E

Certified that the dissertation entitled STUDY OF KINETICS OF ROASTING OF ZINC SULPHIDE which is being submitted by Sri S.Kumar in partial fulfilment of the requirement for the award of Degree of Master of Engineering in Extractive Metallurgy of University of Roorkee is a record of student's own work carried out by him under my supervision and guidance. The matter embodied in this dissertation has not been submitted for the award of any other degree or diploma.

This is further to certify that he has worked for this dissertation for a period of about seven months from January, 1972 to July, 1972.

Roorkee  
August 24, 1972.

*S. K. Gupta*  
(S.K.GUPTA)  
Lecturer in Met. Engineering,  
University of Roorkee  
Roorkee, U.P.

ACKNOWLEDGEMENTS

The author feels pleasure in expressing his sincere gratitude to Sri S.K.Gupta, Lecturer, Metallurgical Engineering Department, University of Roorkee, Roorkee for his invaluable guidance, keen interest and constant encouragement at all times during the preparation of this thesis.

The author's special thanks are due to Dr. M.N. Saxena, Professor and Head of the Metallurgical Engineering Department for providing all the facilities to carry out this investigation.

The author also thanks the staff of Metallurgical Engineering Department for their help and cooperation.

Roorkee  
August 23, 1972.

*A. Kumar*  
Surendra Kumar

P R E F A C E

The roasting of sphalerite concentrate is an important step in the extraction technology of zinc. Roasting is heating to an elevated temperature, without fusion, of ores or metallic compounds in contact with oxidizing materials, in order to produce chemical change or to eliminate a component by volatilization. In Zinc extraction metallurgy, the oxidizing material is oxygen or air and the object is partial or complete elimination of the sulphur in the concentrate.

Most of the Zinc extraction plants used circular multiple hearth furnace of McDougall type for roasting of Zinc sulphide until in 1929 burning concentrate process of roasting of Zinc concentrate was developed. This method, also known as flash or suspension roasting, has the advantages of doubling the furnace capacity with saving in the cost of fuel and production of gases rich enough in sulphur dioxide for acid manufacture. This process was first applied commercially at the Urals chemical plants.

The recent development in the roasting is the use of fluidized bed technique in which the fine solids are transferred into a fluid like state through the contact of gas. In 1944, Dorr-Oliver company acquired

rights to use this technique in the roasting of sulphide ores.

In the present investigation an attempt has been made to study the effects of temperature, porosity, air flow rate and particle size range on the rate of roasting of Zinc sulphide. Influence of the heat liberated during oxidation on the kinetics has been taken into account while determining the rate controlling steps during oxidation.

This thesis has been divided into four Chapters. Chapter- I deals with the general introduction to the subject.

Literature review is included in Chapter-II and deals with the structures of phases formed during oxidation, Zn-S-O system, mechanism and kinetics of oxidation and the influence of various variables on the kinetics of roasting of Zinc sulphide.

Chapter-III gives the description of the experimental set up and procedure followed in the present investigation. The kinetics data were obtained by thermogravimetric technique.

Results obtained from the experiments carried out and a discussion on them constitute the subject matter of Chapter IV. Activation energies during the initial and

subsequent stages are of the order of 12.91 Kcal/g.mole and 3.17 Kcal/g.mole respectively and diffusive steps were found to be rate controlling, throughout the oxidation.

## C O N T E N T S

Chapter		Page
	CERTIFICATE	i
	ACKNOWLEDGEMENT	ii
	PREFACE	iii
	LIST OF FIGURES	vi
	LIST OF TABLES	vii
	LIST OF SYMBOLS	viii
I	INTRODUCTION	1
II	LITERATURE REVIEW	4
	2.1 Introduction	4
	2.2 Crystal structure of Phases formed in roasting	6
	2.3 Zn-S <sub>2</sub> O System	7
	2.4 Mechanism of ZnS oxidation	10
	2.5 Kinetics of Oxidation	12
	2.6 Factors affecting rate of oxidation	20
III	EXPERIMENTAL WORK	25
	3.1 Introduction	25
	3.2 Materials used	25
	3.3 Experimental Set up	26
	3.4 Experimental Procedure	28
IV	RESULTS AND DISCUSSIONS	31
	4.1 Results	31
	4.2 Discussions	32
	CONCLUSIONS	39
	REFERENCES	40
	TABLES I to - XI	43-52

LIST OF FIGURES

- 1 Crystal structure of cubic zinc sulphide
- 2 Crystal structure of zinc oxide
- 3 D.T.A. thermogram of zinc sulphide
- 4 Stable bivariant equilibria in system Zn-S-O at 1100°K
- 5 Rise in temperature of the pellet on the oxidation rate
- 6 Oxidation model of zinc sulphide
- 7-10 Plots of fractional oxidation Versus time at different temperatures, oxygen concentration, porosities and pellet diameters respectively.
- 11(a) Schematic diagram of experimental set up
- 11(b) Design of orificemeter
- 12 General view of experimental set up
- 13,15,17 Experimental plots of fractional oxidation versus time at different temperatures, flow rates, particle size ranges and porosities respectively
- 14 Plot of the rise in temperature of pellet during roasting versus time.
- 18 Photograph of partially roasted zinc sulphide pellet
- 19 Theoretical plot of fractional oxidation Vs fractional thickness
- 20 Plot of fractional thickness versus time
- 21 Plot of  $k$  versus  $1/T$ .
- 22 Plot of square of fractional thickness versus time
- 23 Plot of  $\log k_p$  versus  $1/T$



LIST OF TABLES

- I - V Experimental results of roasting Zinc sulphide at temperatures 800, 850, 900, 950 and 1000°C respectively
- VI Experimental results of roasting of Zinc sulphide at different porosities, air flow rates and particle size ranges.
- VII Values of fractional thickness and fractional oxidation for roasting of zinc sulphide pellet with 'θ' equal to 0.672.
- VIII Specific reaction rate constant values at different temperatures for roasting of Zinc sulphide.
- IX Calculations involved in the determination of theoretical rates of roasting of zinc sulphide
- X Comparison of theoretical and experimentally observed rates of roasting of zinc sulphide
- XI Parabolic rate constant values at different temperatures for roasting of zinc sulphides

LIST OF SYMBOLS

- a height to diameter ratio of the pellet
- A Surface area of the pellet
- $C_{10}$  Concentration of gaseous reactant at the outside surface of the pellet, g moles per litre.
- $C_s$  Concentration of convertible S in ZnS Core,  $\text{g/cm}^3$  of particle volume ( =  $\frac{16}{97.44}$  x density of ZnS)
- $C_p$  Heat capacity of air , Cal/ (g.mole)  $^{\circ}\text{C}$
- $\Delta C$  Difference in concentration of gaseous product  $\text{SO}_2$  at the reaction front and at the exposed surface.
- d diameter of the pellet
- D diffusion coefficient of oxygen in air ,  $\text{cm}^2/\text{sec}$
- $D_T$  diameter of furnace tube
- $D_{\text{eff}}$  effective diffusivity of reactant gas (  $\frac{D_T^2}{\tau}$  )  $\text{cm}^2/\text{sec}$ .
- f fractional oxidation
- $f(\text{CO}_2)$  function of concentration of reactant gas
- $h_{\text{conv}}$  Convective heat transfer coefficient of air,  $\text{g.cal/sec cm}^2 \text{ } ^{\circ}\text{C}$   

$$\left[ h_{\text{conv}} = \frac{k'}{d} \left\{ 2 + 0.69 (Re)^{1/2} (Pr)^{1/3} \right\} \right]$$
- $h_{\text{rad}}$  radiation heat transfer coefficient  

$$\left[ h_{\text{rad}} = 4 \epsilon \sigma (T_G)^4 \right]$$
- $h_{\text{total}}$  total heat transfer coefficient
- $\Delta H^{\circ}$  Heat of oxidation reaction ( $\text{ZnS} \rightarrow \text{ZnO}$ )

- $(J_{SO_2})_{r_0}$  Total flux of species  $SO_2$  expressed with respect to external surface area of particle, gm of  $SO_2 / (cm^2)(sec)$
- $k$  Specific reaction rate constant in surface reaction forming  $ZnO$ ,  $sec^{-1}$  .
- $k_1$  Chemical reaction rate constant per unit area of reacting interface for forward reaction.
- $k_p$  parabolic rate constant  $sec^{-1}$
- $K$  Thermal conductivity of air,  $g.cal/(sec)(cm^2)(^{\circ}C/Cm)$
- $K_s$  Thermal conductivity of  $ZnS$
- $MO_2$  Molecular weight of oxygen, gm
- $n$  Molar quantity of species
- $P$  Absolute pressure, atm.
- $[p_{O_2}]_G$  Partial pressure of oxygen in bulk gas phase atm.
- $R$  Gas constant in mechanical units
- $r$  radius of  $ZnS$  core
- $R'$  Gas constant in heat units
- $r_0$  Radius of pellet
- $t$  time, sec.
- $th$  Fractional thickness
- $v$  Velocity of air in furnace tube,  $cm/sec$ .
- $w$  weight of species
- $X$  Thickness of solid produce layer ( $r_0 - r$ )
- $yo_2$  mole fraction of oxygen
- Subscript b - in bulk gas phase
- o - at the exterior surface of pellet
- i - at  $ZnS/ZnO$  interace.

Greek letters

$\alpha$  Mass transfer coefficient of oxygen, Cm/sec

$$\left[ \alpha = \frac{D}{d} \left[ 2 + 0.69 (Re)^{1/2} (Sc)^{1/3} \right] \right]$$

$\tau$  Tortuosity factor

$\beta$  Labyrinth factor (Viscosity x porosity of sulphide pellet)

$\gamma$  Porosity of product formed (ZnO)

$\mu$  Viscosity of air, poise

$\rho$  Density of ZnS pellet gm/cc

$\rho_a$  Density of air

$\epsilon$  Emissivity of ZnO

$\epsilon_o$  Porosity of oxidised pellet

$\theta_G$  Temperature of reactant gas in bulk gas phase.

$\sigma$  Stefan-Boltzman constant ,  $1.366 \times 10^{-12}$  g.Cal/cm<sup>2</sup> sec °K<sup>4</sup>

$\eta$  Molar rate of oxidation, moles/sec.

$\Gamma$  Diffusive parameter, Cm<sup>2</sup>/sec

$$\left[ \frac{1}{\Gamma} = \frac{1}{[D_{eff}]} + \frac{[po_2]_G \Delta H^2}{RR' (\theta_G)^3 K_s} \right]$$

$\Lambda$  Convective parameter, Cm/sec.

$$\left[ \frac{1}{\Lambda} = \frac{1}{\alpha} + \frac{[po_2]_G \cdot \Delta H^2}{RR' (\theta_G)^3 h_{tot}} \right]$$

Dimensionless quantities

$r^*$  Dimensionless radius ( $r / r_0$ )

Re Reynolds number =  $\left( \frac{\rho_a \cdot v \cdot d}{\mu} \right)$

Sc Schmidt number =  $\left( \frac{\mu}{\rho_a \cdot D} \right)$

Pr Prandtl number =  $\left( \frac{\mu C_p}{K} \right)$

--

CHAPTER - I

## I N T R O D U C T I O N

Roasting processes, which are heterogeneous reaction occurring at the solid-gas interface, are very important because they are employed in the extraction of number of basic metals like Cu, Zn, Pb, Ni, Co etc. The principal object<sup>(1)</sup> of most roasting operations is to oxidize the sulphide particles to oxides or sulphates, which are required for subsequent treatment and to volatilize certain impurities. The oxidation is carried out without fusing the charge. The oxidation of Zinc sulphide falls into this class of reactions.

Of the two processes for extraction of metallic Zinc, namely retort process and electrolytic Zinc process, the latter is superior<sup>(2)</sup> for the reasons of higher recoveries of all metals present and lower operating cost per kilogram of Zinc. In either of the processes, concentrates containing Zinc sulphide must be roasted to convert the Zinc sulphide into Zinc Oxide or Zinc sulphates. Roasting depends almost entirely on the control of temperature and time. The length of the roasting period is usually constant over long periods of time. Therefore, the roasting operation is controlled by temperature.

Roasting processes are highly complicated and there is a lack of knowledge concerning the rate limiting factors, which may strongly depend on temperature, particle size, gas composition and solid structures.

Thorough work has been performed with regard to the structural changes taking place during oxidation and thermodynamics and kinetics of the oxidation reaction<sup>(3-8)</sup>. The thermodynamics gives only an idea of equilibrium conditions or the extent to which the reaction will take place, but it tells nothing about the conditions under which a system will proceed towards equilibrium, not about the mechanism of the reaction. So, it becomes necessary to study the kinetics of oxidation of zinc sulphide.

The kinetics study helps in determining the rate controlling step in the overall reaction; and evaluation of rate controlling step may help in increasing the overall rate of reaction by hastening the rate controlling step.

Since in extraction processes production rates often depend on chemical reaction rates, there are good economic reasons for studying the reaction mechanisms and factors controlling the reaction rates. These factors are physical and chemical



conditions of ore or agglomerate, gas composition, gas pressure and oxidation temperature.

In the present work, an attempt has been made to study the kinetics of oxidation of Zinc sulphide and the effect of various variables, viz, temperature, flow rate of air, particle size of Zinc sulphide and porosity of the pallet. Thermogravimetric technique has been used to study the oxidation kinetics.

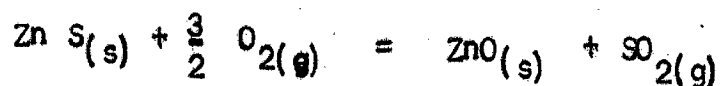
CHAPTER - II

LITERATURE REVIEW

## LITERATURE REVIEW

### 2.1 INTRODUCTION

Oxidation of Zinc sulphide single pallet has been a subject of both experimental and theoretical investigations. The reaction occurring is exothermic and may be considered irreversible. The reaction may be represented as follows :



$$\Delta H_T^{\circ} = -105950 - 0.15 T \text{ cal/g.mole}$$

Zinc sulphide oxidation is a heterogeneous process requiring transport of gaseous oxygen across the porous product layer for continued reaction. It has been found that pallet retains its original dimensions<sup>(4)</sup>.

Various methods have been employed to study the oxidation kinetics of zinc sulphide. One of the earliest and most commonly used is the gravimetric method. Other methods are volumetric, penetration measurement and chemical analysis.

In the thermogravimetric technique<sup>(5,6)</sup>, loss in weight of the sample due to oxidation is recorded with the help of a special balance or some other sensitive weight recording technique. Weight of the hanging sample is recorded after certain intervals of time. The plots of fraction of pellet oxidized versus time may be plotted.

In the volumetric technique<sup>(6)</sup>, rate of evolution of  $\text{SO}_2$  is recorded by absorbing it in slightly acidic N/10 iodine solution. The iodine left after the absorption of  $\text{SO}_2$  is titrated against standard N/10 sodium thiosulphate solution. Thus, the amount of sulphide converted to oxide can be calculated.

In the penetration measurement<sup>(7,8)</sup> technique, the thickness of the oxide shell is measured and fraction of pellet oxidized is calculated by assuming even penetration.

In the chemical analysis technique, the oxidized pellets can be taken out of the reaction chamber at regular intervals of time and are analysed for sulphur to know the extent of oxidation.

## 2.2 CRYSTAL STRUCTURE OF PHASES FORMED IN ROASTING

It has been observed that two phases exist in the oxidation of zinc sulphide in the temperature range  $973^{\circ}$  to  $1300^{\circ}$  K. These are, namely, cubic zinc sulphide and zinc oxide.

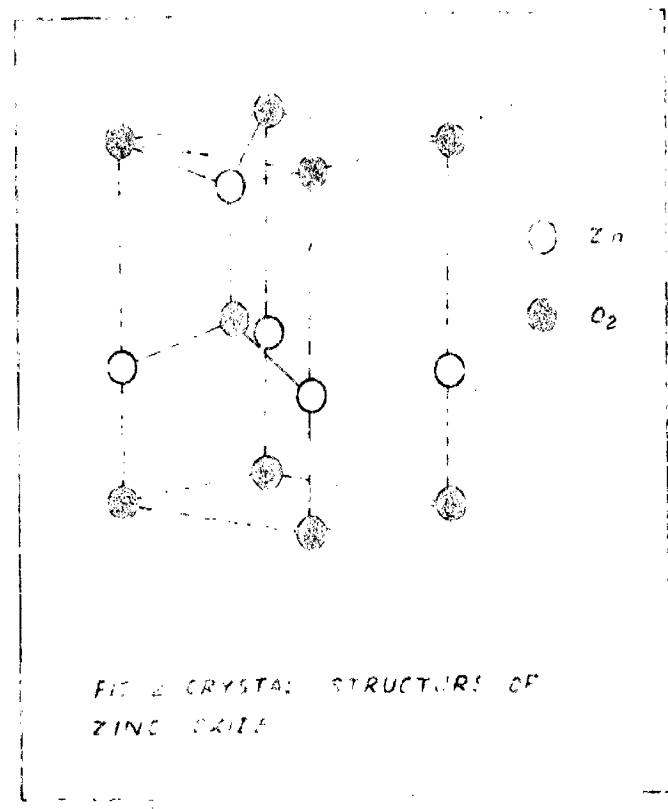
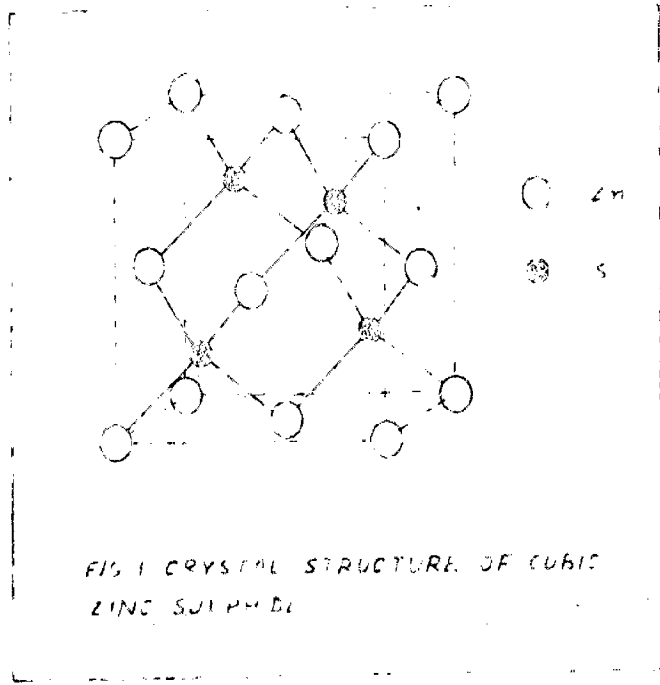
### 2.2.1. Structure of Zinc Sulphide

Zinc sulphide is partially ionic compound. It consists of two F.C.C. Lattices<sup>(9)</sup>, that of zinc and sulphur, of different atomic species interpenetrating so that they are displaced from each other by one fourth of a cube diagonal. Thus, each zinc atom has four sulphur nearest neighbours arranged at corners of a regular tetrahedron. The 12 next neighbours of a zinc atom are all zinc. Zinc sulphide does not have inversion symmetry about its centre. The crystal structure is shown in Fig. 1.

The cubic form of structure with a lattice parameter of  $5.41 \text{ \AA}$  changes to hexagonal form i.e., wurtzite type structure, when zinc sulphide is heated above  $1300^{\circ}$  K.

### 2.2.2 Structure of Zinc Oxide

It consists of wurtzite type structure<sup>(10)</sup>. Zinc atoms are nearly in the positions of hexagonal close

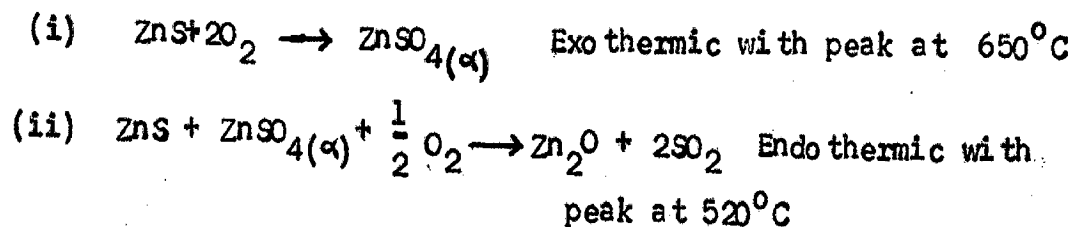


packing. Every oxygen atom lies within a tetrahedral group of four zinc atoms, and these tetrahedral points in the same direction along the hexagonal axis, giving to the crystal its polar symmetry (Fig.2.)

Zinc oxide is anion deficient<sup>(11)</sup> due to the formation of free electrons i.e., non-stoichiometric compound, indicating excess of zinc atoms. Thus zinc oxide can behave as n-type semiconductor. c/a ratio in zinc oxide is  $1.602 \pm 0.00004$ .

### 2.3 Zn-S-O SYSTEM

At low temperatures, however, oxygen may combine directly with sulphide to form sulphate. But some workers<sup>(12,13)</sup> feel that in all cases the sulphate forms first and then decomposes into metal oxide and  $SO_2$  at higher temperatures. This fact has been derived from differential thermal analyser thermogram of ZnS, Fig. 3, and a scheme of reactions has been proposed<sup>(12)</sup>:



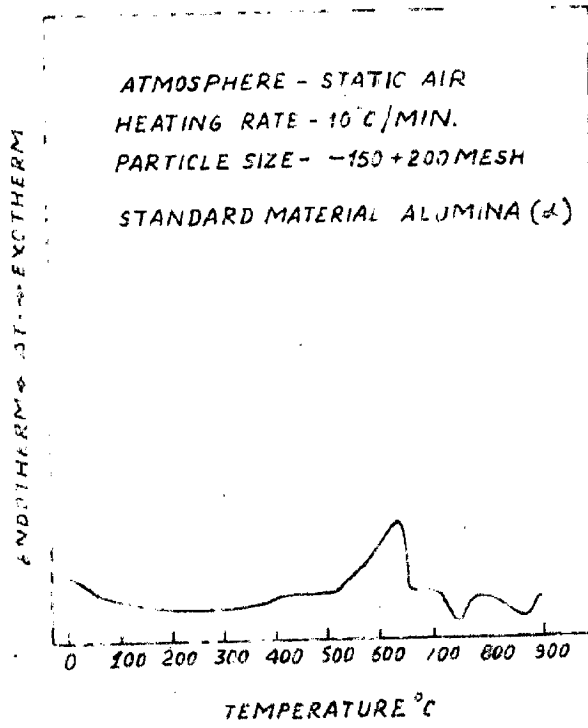


FIG.3 DTA THERMOGRAM OF ZINC SULPHIDE

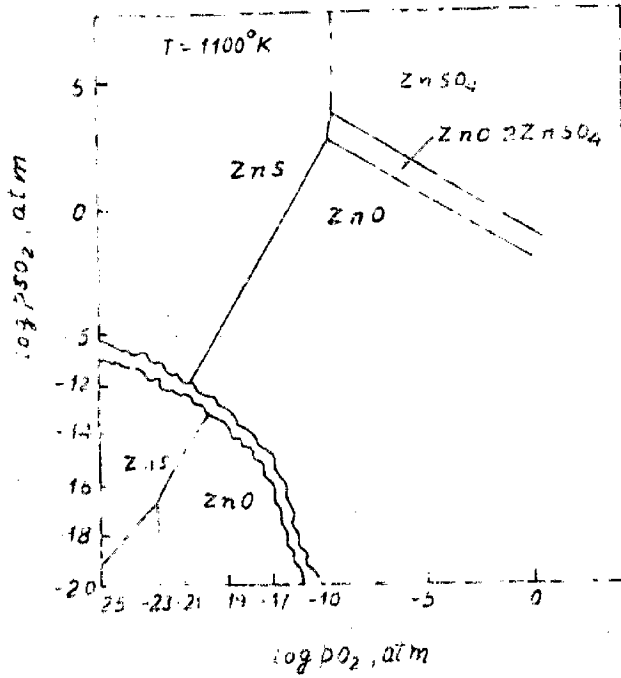
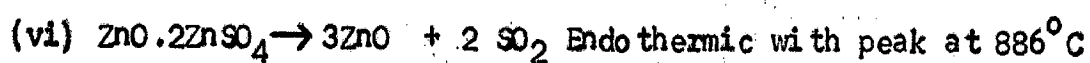
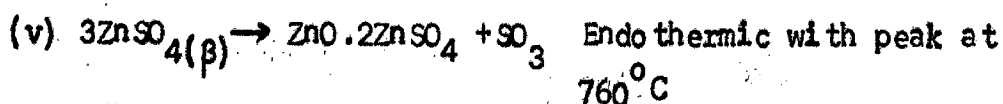


FIG.4 STABLE BIVARIANT EQUILIBRIA IN THE SYSTEM Zn-S-O AT 1100°K





It has been found<sup>(14)</sup> that zinc sulphate decomposes to the extent of 0.05 % only at temperature  $600^\circ\text{C}$ , but in presence of zinc sulphide the decomposition of sulphate is accelerated. The rate of decomposition increases with increasing sulphide: sulphate proportion until it reached to 6 : 1, after which the rate remains essentially constant. The percentage decomposition of sulphate at this proportion is 85%.

The stable bivariant equilibria<sup>(15)</sup> for Zn-S-O system at temperature  $1100^\circ\text{K}$  is shown in Fig. 4. It is obvious that roast reduction type of reactions are not possible in zinc metallurgy as the field of stability of zinc metal is bounded by extremely low values of partial pressures of oxygen and sulphur dioxide. Also, when roaster is operated under conditions of production of small amounts of sulphate in the calcine, the yield contains basic sulphate,  $\text{ZnO} \cdot 2\text{ZnSO}_4$ , not the normal sulphate.

Zn-S-O phase diagram indicates the conditions for the oxidizing or sulphatizing roasting. It is proposed that at higher temperatures or a gas lean in  $\text{SO}_2$  and  $\text{O}_2$  will produce calcine of zinc oxide. Phase diagram clearly indicates the sulphate formation begins when percentage of  $\text{SO}_2$  in gaseous mixture of  $\text{SO}_2$ - $\text{O}_2$  exceeds 6.54% and the rate of formation of sulphate, which is proportional to the amount of  $\text{SO}_3$  present in the system at the equilibrium condition, becomes maximum at 64%  $\text{SO}_2$  in mixture<sup>(6)</sup>.

At temperatures above  $1100^\circ\text{C}$ , Zinc sulphide vaporizes<sup>(16)</sup> and the vapors are oxidized to zinc oxide. The structure of this oxide is different from that obtained at lower temperatures<sup>(7)</sup>. The porous structure which would otherwise have been formed is being filled in by the deposition of oxide by the vapour phase reaction.

Transition from cubic sphalerite to hexagonal wurtzite takes place at temperature  $1300^\circ\text{K}$ . Rate of oxidation reaches maximum at this temperature. A further increase in temperature leads to a decrease in reaction capability<sup>(17)</sup> of the sulphide at the expense of the formation of dense reaction product layers which grow on the high temperature wurtzite-phase base.

In the oxidation of zinc sulphide at temperatures, above  $900^\circ\text{C}$ , penetration becomes very uneven over different

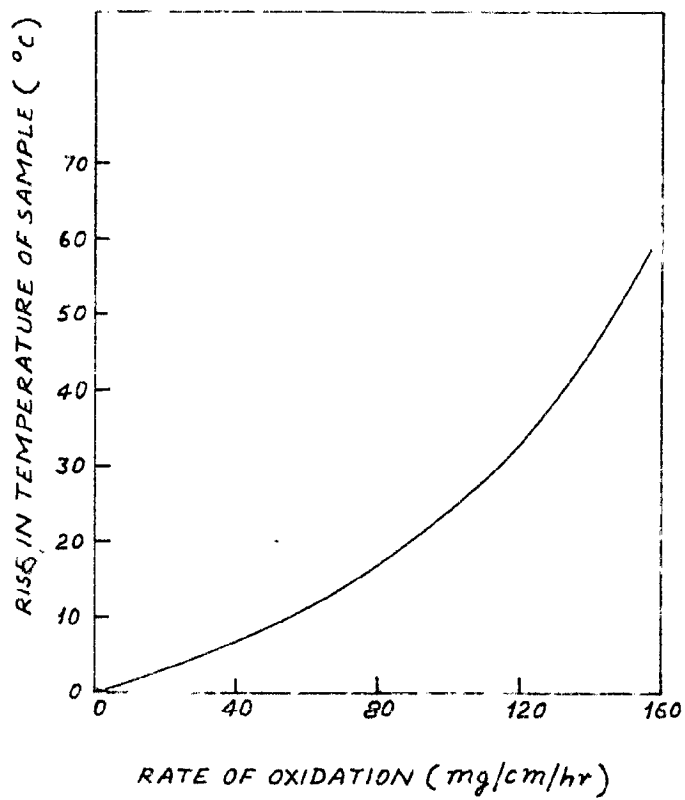


FIG.5 DEPENDENCE OF RISE IN TEMPERATURE OF SAMPLE ON ITS OXIDATION RATE.

parts of the pellet. This is explained due to thermal instability. The thickness of oxide layer impedes the escape of the heat of reaction which thereby causes a local rise in temperature and results in local increase in rate of oxidation<sup>(6)</sup>.

But, now it has been shown that increase in temperature is normal and a thermally instable situation within the particle of zinc sulphide does not arise<sup>(18)</sup>. A maximum temperature rise of  $27^{\circ}\text{C}$ , for a particle of 1.0 cm dia oxidised at  $961^{\circ}\text{C}$ , has been found experimentally which is in very good agreement with the computed value obtained from a mathematical model. Also, it has been found that rise in the interface temperature varies linearly<sup>(6)</sup> with the rate of oxidation of samples as shown in Fig. 5.

#### 2.4 MECHANISM OF ZnS OXIDATION

Oxidation reaction in case of zinc sulphide has been found to proceed in a topochemical manner<sup>(5)</sup>. In other words, as the reaction proceeds, a progressively increasing thickness layer of zinc oxide is formed on the outer surface of the sample at the expense of zinc sulphide. The generalized model for gaseous oxidation of zinc sulphide is illustrated in Fig. 6. It shows a partially oxidized sphere of zinc sulphide in a gas

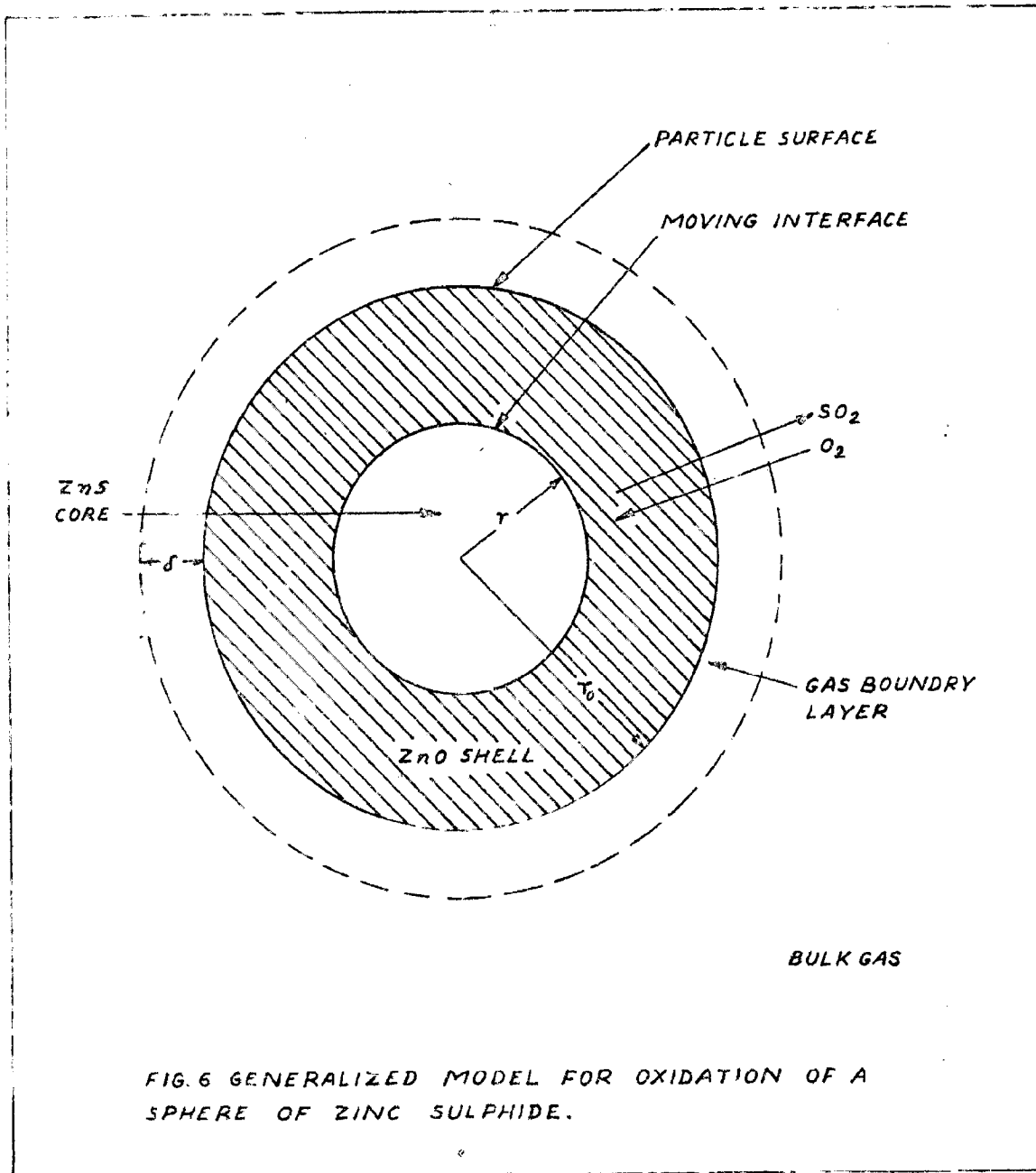
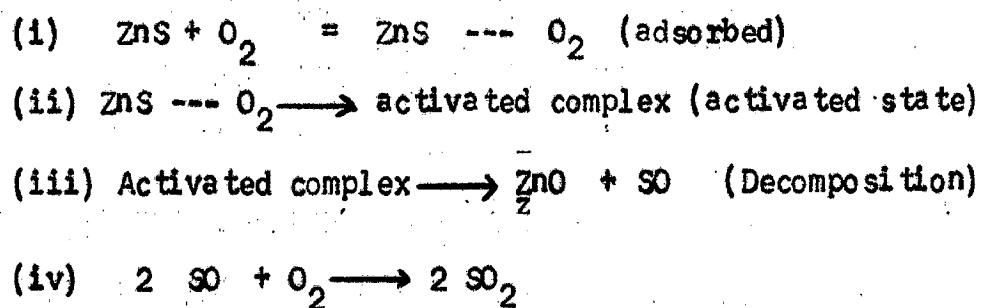


FIG. 6 GENERALIZED MODEL FOR OXIDATION OF A SPHERE OF ZINC SULPHIDE.

stream surrounded by a stagnant boundary layer of gas.

At the ZnS/ZnO interface, reaction mechanism probably occurs in several stages. The oxygen is first adsorbed on to the surface of sulphide, forms activated complex and then decomposes to Zinc oxide and  $\text{SO}_2$ . The overall mechanism for the oxidation of ZnS may be represented as follows :



This postulate suggests that SO exists<sup>(19)</sup> as an intermediate product and the formation of activated complex, step 2, is the rate controlling.

According to second theory<sup>(13)</sup>, adsorbed oxygen on to the surface of sulphide results in the formation of sulphide complexes  $\text{ZnSO}_3$ ,  $\text{ZnSO}_4$  and dissociation of these into ZnO and  $\text{SO}_2$  without formation of any activated complex.

The third theory<sup>(20)</sup> suggests that adsorbed oxygen yields electrons and becomes incorporated in the lattice of the mineral. The electrons neutralize the sulphide ions on the nearby surface as it unites with

another oxygen molecule adsorbed besides it. The  $\text{SO}_2$  molecule so formed desorbs and migrates away leaving a vacant site on the surface. Another sulphur ion may move to occupy this site and continue the reaction, but in general the interface advances into the mineral to reach more sulphur ions.

The velocity of reaction is presumably governed by the number of oxygen molecules adsorbed per unit area of interface and in accordance with the laws of adsorption, rate is proportional to the value of partial pressure of oxygen in the atmosphere round the particle. It is obvious that higher overall reaction rates can be obtained by increasing the reaction interface area. This can rapidly be done by reducing the size of the ore particle.

## 2.5 KINETICS OF OXIDATION

Rate equation for a irreversible heterogeneous reaction of a gas with a solid has been derived by Lu<sup>(21)</sup> considering contributions of chemical reaction at inter-phase boundaries and diffusion through the solid product layer simultaneously. The equation is given as,

$$\left(\frac{C_{10}}{R_p}\right)^{\frac{1}{2}} = \frac{x}{k_1} + \frac{1}{2 D_{\text{eff}}} x^2 \quad (1)$$

In the derivation of the above rate equation, the diffusion rate of gaseous product was not considered<sup>(22)</sup>. Of the two terms on the right hand side of rate equation, the first represents the contribution of interfacial chemical reaction and the second that of gaseous diffusion.

#### 2.5.1 Rate Controlling Step in Oxidation

The reaction of zinc sulphide with oxygen is a heterogeneous reaction involving several phases among which reactants and products are distributed. All reactions occurring at the surface of zinc sulphide particle can be divided into following steps :

- (i) Transfer of reactant gas (oxygen) from the bulk gas stream across the gas boundary layer to the exterior surface of the pellet and the reverse transfer of the product gas ( $\text{SO}_2$ ).
- (ii) Diffusion and bulk flow of oxygen from the pellet surface through the product shell ( $\text{ZnO}$ ) onto the  $\text{ZnS}/\text{ZnO}$  interface and reverse transfer of  $\text{SO}_2$ .
- (iii) Chemical reaction at the interface, which results in consumption of oxygen gas and generation of  $\text{SO}_2$  gas and heat, at the same time the  $\text{ZnS}$  core is consumed and thickness of  $\text{ZnO}$  shell increases.



It is obvious that rates are dominated by widely different factors in addition to the temperature gas composition and concentration gradient involved. Slowest step among these controls the overall rate of oxidation. The following assumptions<sup>(5)</sup> are made in evaluating the rate controlling step :

- (i) The increase in temperature of interface is neglected i.e., no temperature gradient exists within the particle.
- (ii) Reaction proceeds symmetrically, i.e., reagent and product transfer rates are spherically symmetrical.
- (iii) An average porosity and permeability can be assigned to the product layer, i.e., the densification and growth of ZnO crystals in the oxidized shell are neglected.
- (iv) Product layer has no catalytic effect on the reaction.
- (v) Oxidation is pictured as being Quasi Steady-State.

The quas-i steady-state assumption permits that the product generation rate may be related to the

reactant consumption rates. For oxidation reaction, the rate may be defined as,

$$-\left(\frac{dn}{dt}\right)_{\text{ZnS}} = -\frac{2}{3} \left(\frac{dn}{dt}\right)_{\text{O}_2} = \left(\frac{dn}{dt}\right)_{\text{ZnO}} = \left(\frac{dn}{dt}\right)_{\text{SO}_2}$$

The oxidation rate may be related to the rate of conversion of ZnS to ZnO, i.e. weight loss, by the following equation,

$$\left(\frac{dn}{dt}\right)_{\text{ZnS}} = \frac{1}{16} \left(\frac{dw}{dt}\right) \quad (\text{ii})$$

The analysis of the various rate controlling steps is given below :

(i) Gaseous Film Resistance - A stagnant boundary layer of gas is formed around the sulphide particle and this layer offers a resistance to the gaseous reactant and product to come at the surface of the oxide from the main gas stream and vice versa. Therefore, the rate controlling step is called 'Gaseous film resistance'. Mass transfer to and from the surface of the pallet occurs simultaneously by molecular diffusion and convection mechanism.

For spherical pallet, rate of conversion of ZnS to ZnO is given as,

$$\left(\frac{dW}{dt}\right) = C_s \cdot 4 \pi r^2 \left(\frac{dr}{dt}\right) \quad (\text{iii})$$

And, fractional oxidation 'f' is defined as,

$$f = \frac{\text{sulphur converted to oxygen}}{\text{Total sulphur}} = 1 - \left(\frac{r}{r_0}\right)^3$$

$$= \alpha \frac{P.M_{O_2}}{r_0 C_s \cdot R_1 T} \left[ y_{O_2}^{(b)} - y_{O_2}^{(0)} \right] t \quad (\text{iv})$$

In the above equation, the mass transfer coefficient, the pallet radius and concentration of sulphur are approximately independent of time and thus a plot of 'f' versus 't' should give a straight line if gaseous film resistance is the rate controlling step.

The rate of oxidation based on step (i) depends on flow characteristics of the system, such as the mass velocity of the fluid stream, the size of the pallet and diffusional characteristics of the fluid involved.

(ii) Shell Layer Resistance - According to this the diffusion of the gaseous reactant and product through ZnO layer is the rate controlling step. The diffusion across the product phase, ZnO, may take place by either molecular or knudsen gaseous diffusion through the pores of oxidized shell. Rate of weight loss of ZnS pallet, as derived by Jost<sup>(23)</sup> using mathematical formulation, is given below :

$$\left( \frac{dW}{dt} \right) = \pi r_o^2 (J_{SO_2})_{r_o} \quad (v)$$

Rate based on step (ii) depends on degree of porosity of product shell, the dimensions of the pores, the extent to which they are interconnected, the size of the pellet, the thickness of product shell and the diffusional characteristics of the system.

(iii) Interface Resistance- Chemical reaction occurring at the interface is the rate controlling step. The process of oxidation is thermally activated and for this activation energy is required to continue the reaction.

The rate of consumption of oxygen and formation of sulphur dioxide due to chemical reaction is proportional to the area of the receding interface. The rate of weight loss is given as follows :

$$-\left( \frac{dW}{dt} \right) = \frac{32}{3} k_r (4 \pi r^2) f \left[ C_{O_2}^{(i)} \right] \quad (vi)$$

The following equation is also true in case of chemical reaction rate controlled, which is derived from equation (vi),

$$\left[ 1 - (1-f)^{1/3} \right] = \frac{32}{3} \frac{k_r}{C_s \cdot r_o} f \left[ C_{O_2}^{(b)} \right] t \quad (vii)$$

Thus a plot of  $[1 - (1-f)^{1/3}]$  Vs 't' should yield a straight line if the chemical reaction at the interface is the rate controlling step for the process.

The rate based on step (iii) depends on the activation energy for the process, the mechanism of reaction and the interface area available for the reaction.

Thus the oxidation of ZnS is either diffusion controlled or chemical reaction controlled, because gaseous film resistance plays role no more once a 'plateau' is established<sup>(24)</sup>. After this 'plateau' region rate is virtually independent of gas velocity.

It was believed earlier that oxidation of ZnS was chemically controlled<sup>(7)</sup> at lower temperatures upto 830°C. The oxidation rate was found to be linear except at higher temperatures where the experimental value came less than that of predicted by calculations. This was attributed as either diffusion controlled or the self heating<sup>(6)</sup> of the pallet at the reaction interface. This idea was also confirmed by the fact that above 830°C, corners of ZnS crystal began to show a rounding and penetration became uneven<sup>(7)</sup>. This is clearly what would be expected if the diffusion of

oxygen or sulphur dioxide through the oxide layer was becoming significant as a rate controlling factor. Activation energies obtained by different workers from the Arrhenius plot of these rates are given below :

Activation energy	Author
50.0 KCal/g. mole	Cannon & Denbigh <sup>(7)</sup>
57.5 KCal / g.mole	Dimitrov & Paulin <sup>(13)</sup>
60.3 KCal / g.mole	Ong, Wadsworth and Fassell <sup>(6)</sup>

But , now it has been confirmed by various workers that process of oxidation of ZnS is predominantly controlled by shell layer transport at the temperatures above 700°C . The activation energy values found out by various workers are given below :

Activation Energy	Author
2.9 KCal/g.mole	Rao and Abraham <sup>(8)</sup>
3.0 KCal/g.mole	Denbigh & Beveridge <sup>(4)</sup>
3.5 KCal/g.mole	Gerlach, Stichel & Erzbergbau <sup>(25)</sup>

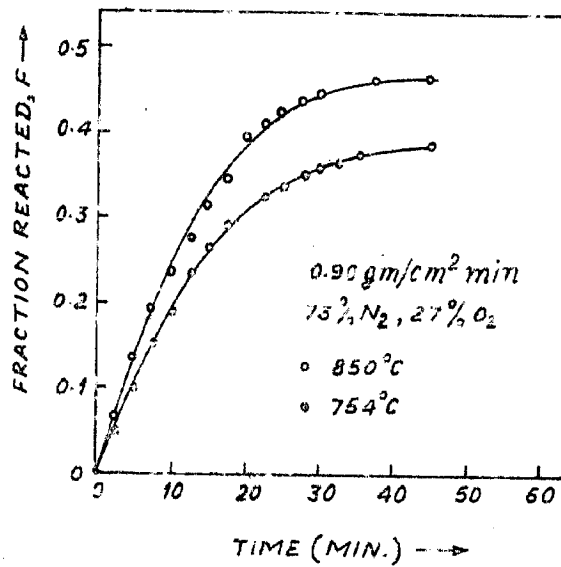


FIG. 7 PLOT OF FRACTION REACTED VS TIME FOR PELLETS OF 1.25 CM DIAM. AT 850°C & 754°C WITH ALL OTHER PROCESS VARIABLES THE SAME.

## 2.6 FACTORS AFFECTING RATE OF OXIDATION

The kinetics of oxidation of ZnS is markedly influenced by the process variables such as temperature of oxidation, gas flow rate, oxygen concentration, porosity and particle size, size of the pallet and impurities present in Zn ore. The role played by these process variables is discussed below.

### 2.6.1. Effect of Temperature

Oxidation of Zinc sulphide is a thermally activated process, therefore, the rate of oxidation increases with increase in temperature<sup>(5)</sup>. By increasing the temperature diffusion rate is increased. The effect of temperature on the fractional oxidation, i.e., oxidation rate, is shown in Fig. 7. Increase in fraction oxidized is less in the early stages than in the later stage with increasing temperature. This is attributed to the fact that ZnO shell grows thicker with time and the porosity of ZnO is more than that of ZnS.

### 2.6.2 Effect of Gas Flow

When the flow rate is low the reaction rate is found to be strongly dependent on the velocity of gas. Increasing flow rate increases the reaction rate till a plateau is established and after that the reaction rate is virtually independent of gas velocity<sup>(24)</sup>.



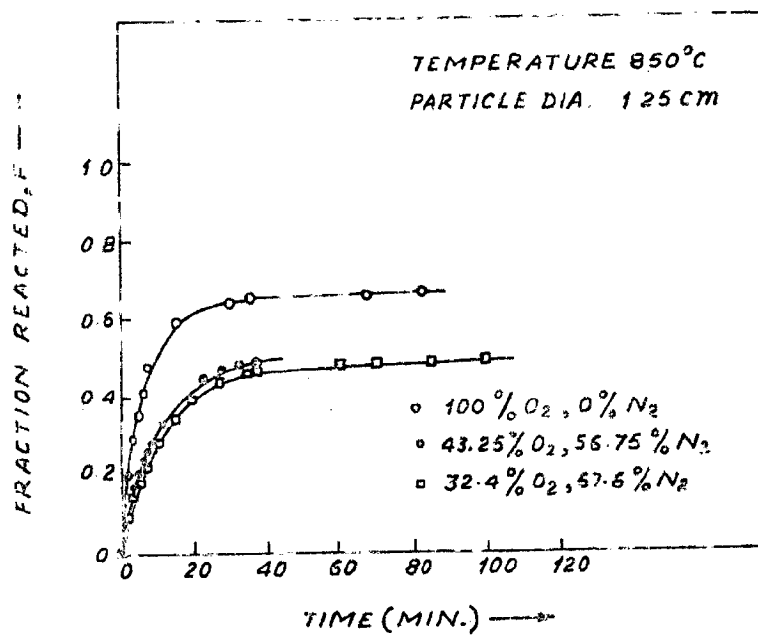


FIG 8 FRACTION REACTED VS TIME PLOTS FOR PELLETS REACTED IN DIFFERENT O-N GAS MIXTURES.

Thus, it may be concluded that by increasing the 'air factor'; which is ratio of air supplied to stoichiometric amount of air, within the 'plateau' region, the rate of oxidation increases<sup>(26)</sup>. It has been found that increasing the flow rate of air than required for stoichiometric amount of 7.20 litres/hr for 5 gm sample having 31.92% S has negligible effect on the rate of oxidation<sup>(27)</sup>.

#### 2.6.3 Oxygen Concentration

Studies of rate of oxidation as a function of oxygen concentration have indicated<sup>(6)</sup> primary single site adsorption followed by decomposition of surface sites. The absolute rate of reaction depends on the ratio of number of reactive sites covered by oxygen to the total number of reactive sites. As the oxygen concentration in  $O_2 - N_2$  gas mixture is increased, the number of covered sites on the surface in a given time increases and rate of reaction increases as shown in Fig. 8.

#### 2.6.4 Porosity and Particle Size

Other factors remaining constant, rate of oxidation increases with increase<sup>(5)</sup> in porosity

and decrease in particle size. Increased porosity facilitates diffusion while smaller particles offer more surface area. The effect of porosity on the fractional oxidation is shown in Fig. 9. The following equation explains the significance of porosity on the rate of conversion of ZnS to ZnO.

$$\left(\frac{dn}{dt}\right)_{\text{ZnS}, d} = D A \epsilon_0 \beta \frac{\Delta C}{x} \quad (\text{viii})$$

Thus the rate of oxidation is directly proportional to the porosity.

#### 2.6.5 Pellet Diameter

It has been found that under same experimental conditions of temperature, gas composition and so forth, the smaller the pellet size, faster will be the complete conversion<sup>(5)</sup>, Fig. 10. This is attributed to the fact that in smaller pellets diffusion path becomes less.

#### 2.6.6 EFFECT OF IMPURITIES

Main impurities commonly found with Zn ore are  $\text{As}_2\text{S}_3$ ,  $\text{FeS}$  and  $\text{SiO}_2$ . Both  $\text{SiO}_2$  and  $\text{Fe}_2\text{O}_3$  which are almost always present in roasting operation act as catalysts and promote the following reaction.

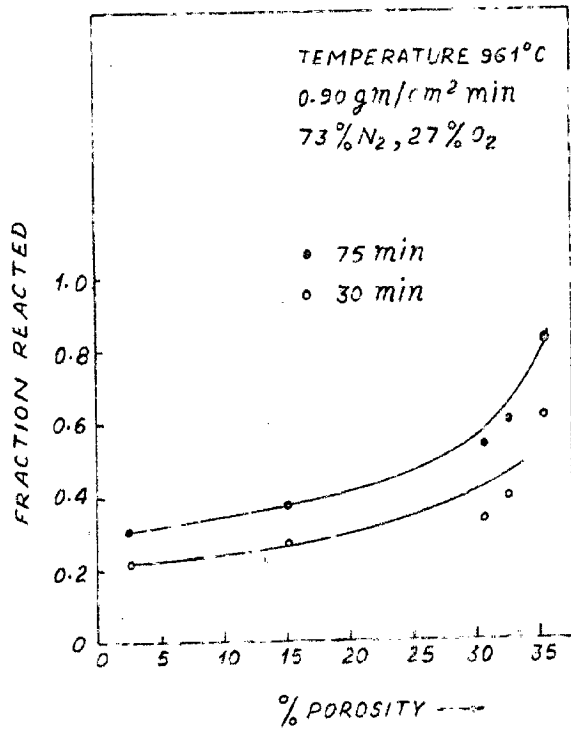


FIG 9 PLOT OF FRACTION REACTED VS  
 PERCENT POROSITY WITH THE TIME OF  
 REACTION AS A PARAMETER.

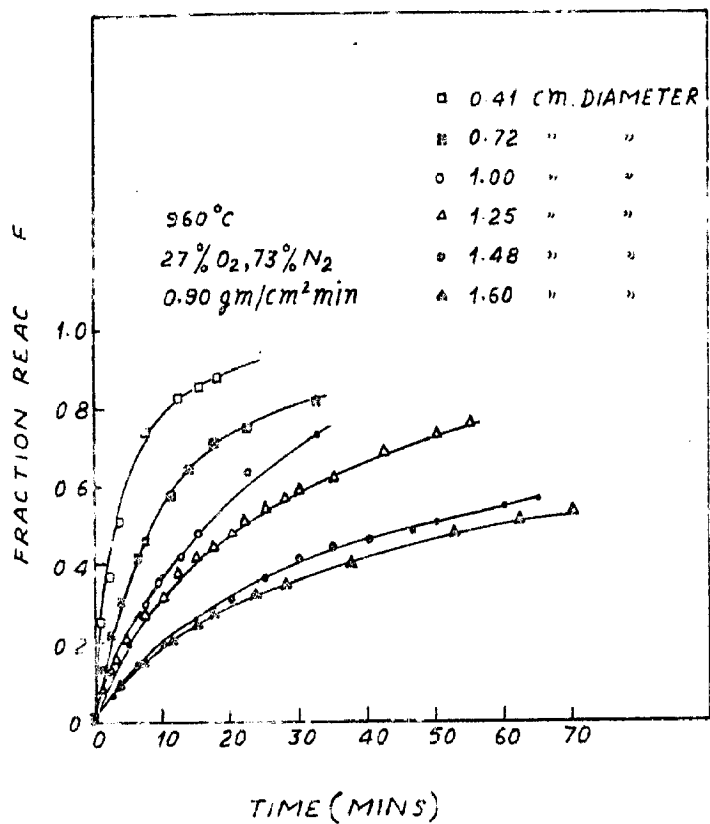
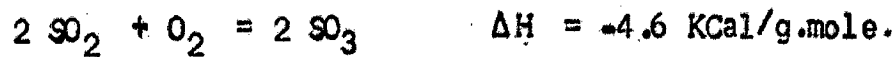
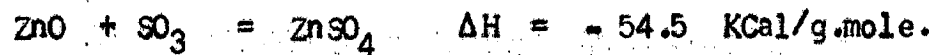


FIG 10 PLOT OF FRACTION REACTED VS TIME FOR  
 PELLETS OF VARIOUS INITIAL DIAMETERS UNDER  
 THE SAME EXPERIMENTAL CONDITIONS.



So, some of the  $\text{SO}_2$  formed by burning of sulphur combines with  $\text{O}_2$  to form  $\text{SO}_3$ . Thus formed  $\text{SO}_3$  in turn reacts with  $\text{ZnO}$  to form  $\text{ZnSO}_4$ .



Whether the sulphate will form or not depends upon :

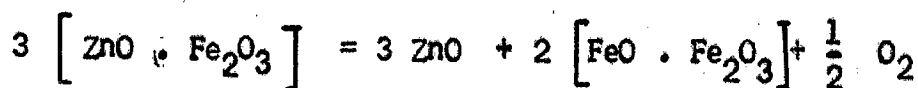
- (i) the partial pressure of  $\text{SO}_3$  in roaster gases,
- (ii) the temperature, which determines dissociation tension of sulphate. Any sulphate will form only when partial pressure of  $\text{SO}_3$  is greater than dissociation tension of sulphate. Formation of sulphate is promoted by low roasting temperatures and high  $\text{SO}_3$  concentration. At high temperatures, sulphate decomposes to  $\text{ZnO}$  and  $\text{SO}_3$ .

It has been found<sup>(8)</sup> that when Fe is upto 5% in  $(\text{ZnS} + \text{FeS})$  compacts, oxidation rate is not affected whereas 10% Fe as FeS lowers the oxidation rate considerably and formation of ferrite takes place. Formation of Zinc ferrite is enhanced with the increase of flow rate of air above the stoichiometric amount<sup>(27)</sup>

Therefore, atmosphere prevailing in the roaster should be slightly oxidizing or neutral.

Amount of zinc ferrite is negligible when oxidation temperature is lower than  $650^{\circ}\text{C}$ , but it rapidly increases above  $650^{\circ}\text{C}$ . Zinc ferrite formed at temperatures above  $650^{\circ}\text{C}$  is insoluble<sup>(28)</sup> in the weak, spent electrolyte ( 200 gm per litre  $\text{H}_2\text{SO}_4$  ) normally used as the solvent in the electrowinning of Zinc and Zinc thus tied finds its way into the leach residue.

There is a tendency towards decreased formation of ferrite at the higher roasting temperatures. The conversion of iron to zinc ferrite is 14 percent lower at  $1150^{\circ}\text{C}$  than at  $950^{\circ}\text{C}$ . The scant data on the properties of zinc ferrite prevents a thermodynamic prediction of the reactions involved, and the mechanism is suggested to be replacement of zincite by ferrous oxide,



Silica present in the ore forms Zinc silicate,  $\text{Zn}_2\text{SiO}_4 \cdot \text{H}_2\text{O}$ , which forms silicic acid on reacting with  $\text{H}_2\text{SO}_4$  and hampers filtration and ~~sinking~~<sup>settling</sup> during subsequent operations. Zinc silicate formation is minimized by using  $\text{O}_2$  enriched air as this shortens the total oxidation time<sup>(29)</sup>.

CHAPTER III

EXPERIMENTAL WORK



## EXPERIMENTAL WORK

### 3.1 INTRODUCTION

As already stated, several methods are available for studying the roasting kinetics of sulphide minerals, having their own merits and demerits. In the present work thermogravimetric technique has been employed with the help of single pan balance with certain modifications having sensitivity of the order of 0.1 mg. This method has the following advantages,

- (i) single pallet is required for each run ,
- (ii) it consumes lesser time for each experiment,
- (iii) this method is more accurate than any other.

### 3.2 MATERIAL USED

Zinc sulphide in the form of powder of commercial purity was used to carry out the present investigation.

The powder analysis is as under

Zn	65.41 wt %
S	33.15 "
Fe	0.91 "

This zinc sulphide<sup>(30)</sup> was heated at 450°C for 4 hours to convert FeS present in it to Fe<sub>2</sub>O<sub>3</sub>. After heating, the powder analysis is as under

Zn	- 65.52 wt. %
S	- 32.60 "
Fe	- 0.93 "

### 3.3 EXPERIMENTAL SET UP

The schematic diagram of the experimental set up used to carry out the work is shown in Fig. 11a., and the general view is shown in Fig. 12. It consists of following parts .

- (a) Air compressor
- (b) Drying and Purifying unit
- (c) Flowmeter with manometer
- (d) Preheater
- (e) Reactor
- (f) Balance

#### 3.3(a) Air Compressor

Air required for oxidation of zinc sulphide pallet was supplied by an air compressor. The rating of the compressor was :

$$\text{H.P.} = 1$$

$$\text{r.p.m.} = 750$$

$$\text{Max. pressure} = 5.2725 \text{ Kg/cm}^2$$

#### 3.3(b) Drying and Purifying Unit

It consisted of two separate units, one for air drying which consisted of three bottles specially built for this purpose, having concentrated  $\text{H}_2\text{SO}_4$ , anhydrous  $\text{CaCl}_2$  and third empty, and one for nitrogen purification which consisted of two bottles, one filled

1. DRYING AND PURIFICATION
2. CONTROL VALVE
3. ORIFICE METER
4. TWO WAY VALVE
5. PREHEATER
6. REACTOR
7. THERMOCOUPLE (TEMPERATURE)
8. THERMOCOUPLE (TEMPERATURE)
9. SINGLE PAN BALANCE
10. WOODEN PLATFORM

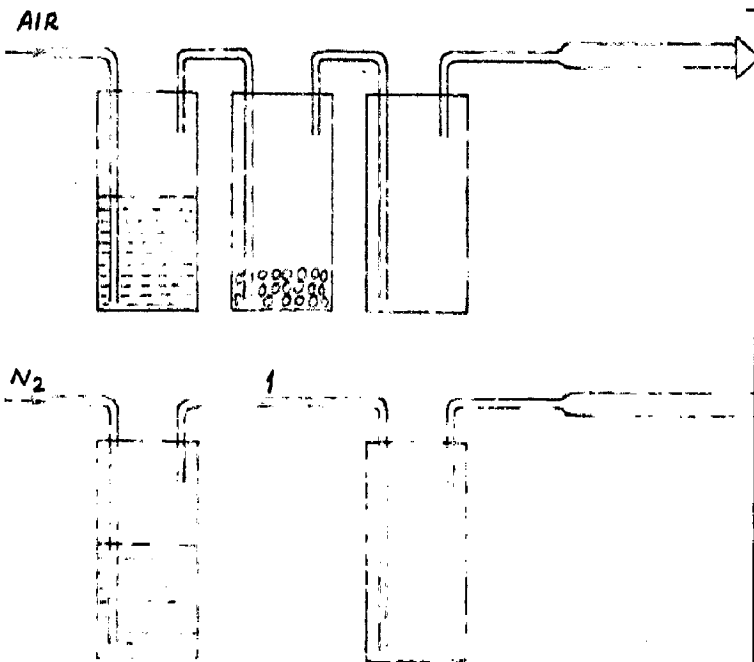
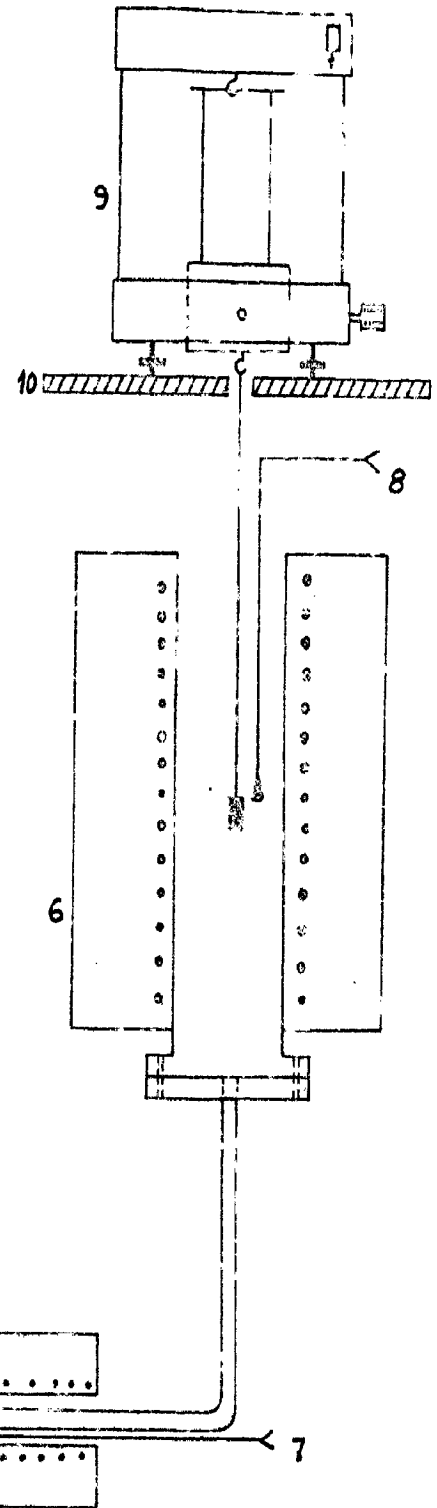


FIG. 11(a), SCHEMATIC DIAGRAM

1. DRYING AND PURIFICATION UNIT
2. CONTROL VALVE
3. ORIFICE METER
4. TWO WAY VALVE
5. PREHEATER
6. REACTOR
7. THERMOCOUPLE (TEMPERATURE OF PREHEATER)
8. THERMOCOUPLE (TEMPERATURE OF REACTOR)
9. SINGLE PAN BALANCE
10. WOODEN PLATFORM

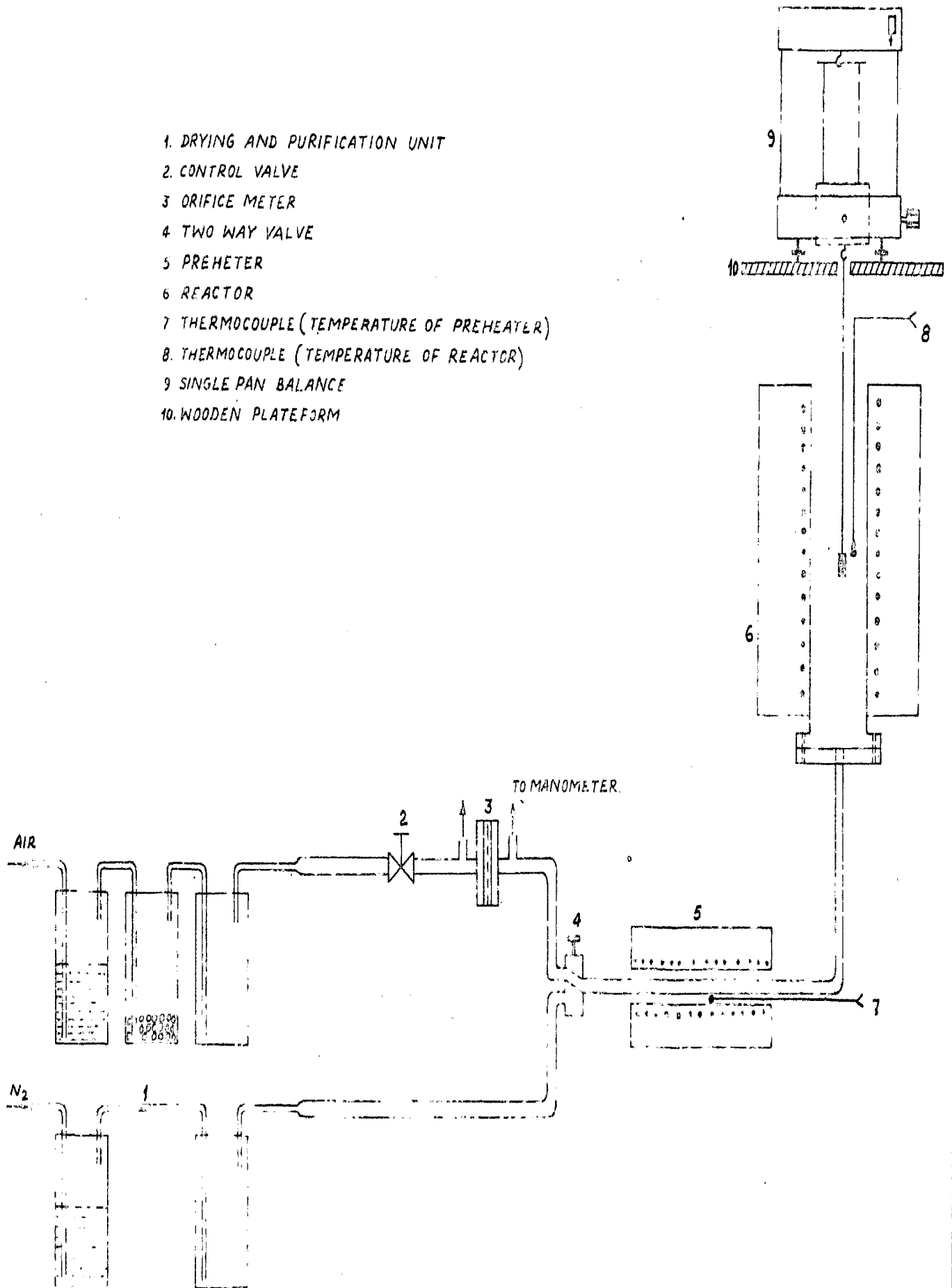


FIG. 11(2), SCHEMATIC DIAGRAM OF EXPERIMENTAL SETUP

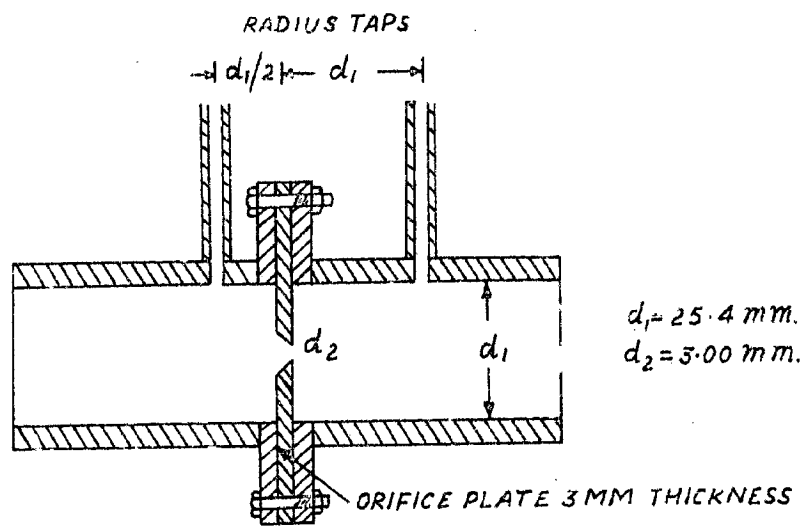


FIG. 11(b) DESIGN OF THE ORIFICE METER

with alkaline pyragalloi for removal of oxygen and other empty. The empty bottles were placed at the end of each unit to prevent substances contained in previous tubes from going into the preheating furnace.

### 3.3(c) Flowmeter with Manometer

The air flow rate was measured with the help of an orificemeter which was calibrated against a wet gas flow meter. The design of the orificemeter is shown in Fig. 11(b). Manometer was placed at an angle of  $30^{\circ}$  from horizontal.

### 3.3(d) Preheater

It consists of a mild steel tube of 1.25 cm diameter and overall length of 150 cm placed in a sillimanite tube furnace of 2.54 cm internal diameter. The temperature in the tube was controlled by chromel-alumel thermocouple and energy regulator within the limits of  $\pm 5^{\circ}\text{C}$ .

### 3.3(e) Reactor

The furnace tube was of alumina, having internal diameter 5 cm and overall length 90 cm. The winding was done by 18 SWG Kanthal wire. The resistance of the furnace was 25 ohms. The alumina tube was then kept in a cylindrical steel shell of dimensions 45 cm diameter and 60 cm length and the space between the tube and shell

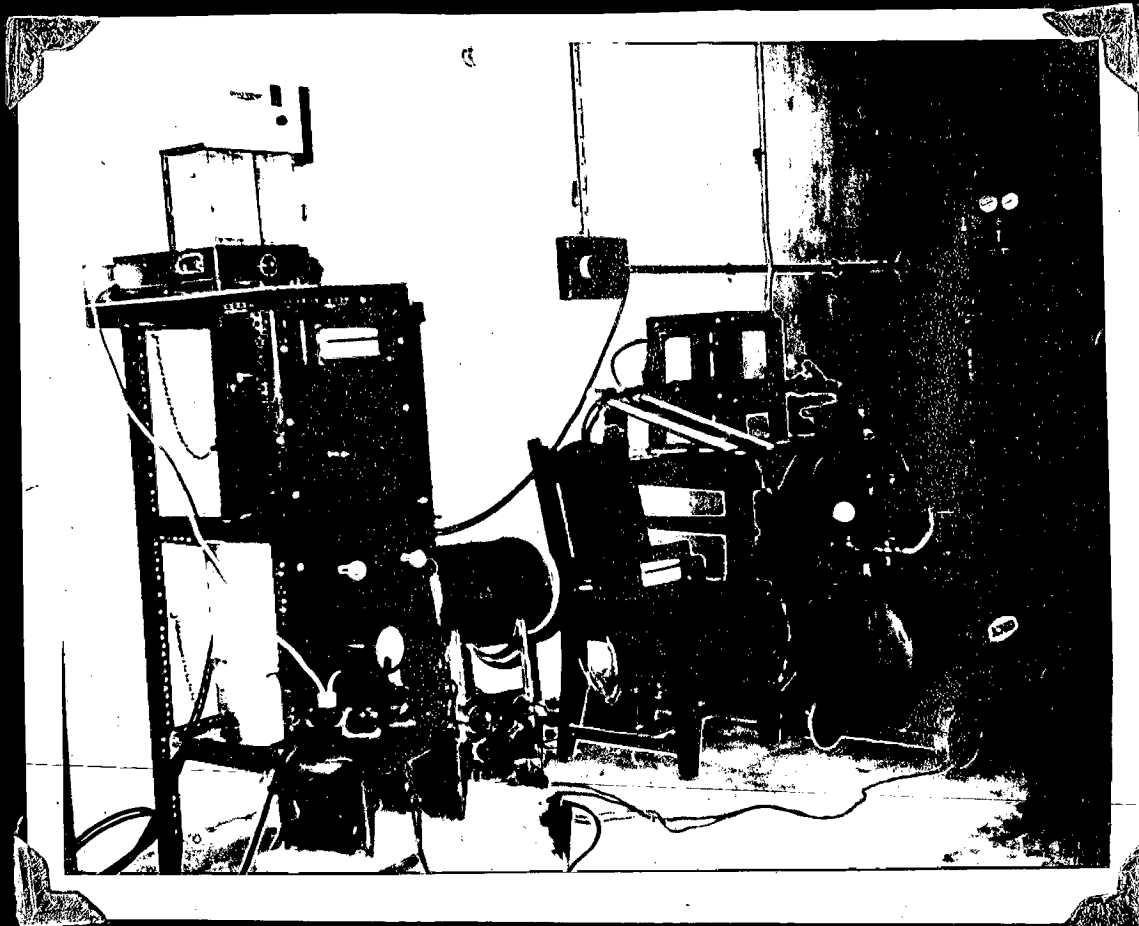


Fig.12. GENERAL VIEW OF EXPERIMENTAL SETUP.

was then packed with asbestos powder. The ends of the shell were then closed by nuts and bolts.

The temperature of the furnace was measured by a Pt - Pt/13% Rh thermocouple inserted into the furnace tube from the top end. Bare end of the thermocouple was about 0.5 cm above the upper end of the sample and about 1.5 cm away from the centre line of the alumina tube. The temperature control was maintained within the limits of  $\pm 5^{\circ}\text{C}$  over a 15 cm central zone by means of a Sunvick energy regulator.

### 3.3(f) Balance

The balance used was a single pan analytical balance, owa Labor-type 707.04, specially modified so that the pallet can be suspended by a thin platinum wire from the pan of the balance. The balance was one of the aperiodic projection type, reading upto 100 mg on the illuminated scale to a sensitivity of 0.1 mg. The zero of the balance was checked after each run of the experiment.

## 3.4 EXPERIMENTAL PROCEDURE

Various steps involved in the procedure are described below :

### 3.4.1. Pellet Making -

The heated powder, free from any FeS, was ground



to a size of  $-100 +240 \#$  and was pressed in a die of 1.55 cm internal diameter at a constant load of 3 tons for 2 minutes. The pellets were then heated at  $200^{\circ}\text{C}$  for 2 hours to remove water and lubricating oil adhered on the surface. Now porosity measurements were done. Porosity of these pellets were also determined.

#### 3.4.2 Roasting of Zinc Sulphide Pellets

The roasting studies were carried out by suspending the pellet in the reactor at the required temperature. The reactor was flushed by nitrogen for 5 minutes before introducing the pellet. The preheating furnace was heated at temperature  $25^{\circ}\text{C}$  less than prevailing in the reactor. Pellet was heated for next 10 minutes in nitrogen atmosphere to bring it at the required oxidation temperature.

Now, nitrogen supply was put off and air was passed from air compressor at a rate of 500 cc per minute. Oxidation began and the loss in weight of the pellet was noted at regular intervals of time. When oxidation was nearing completion i.e., negligible weight loss, air supply was put off and pellet was cooled and taken out. The above procedure was repeated with different variables of interest such as temperature, flow rate of air, porosity of the pellet and particle size range of the pellet.

The rise in the temperature of interface ZnS/ZnO was noted at different temperatures of oxidation by placing a Pt-Pt/13% Rh thermocouple in the small groove made in the side of the pellet.

CHAPTER IV

RESULTS AND DISCUSSIONS

## RESULTS AND DISCUSSIONS

### 4.1 RESULTS

The experiments for the oxidation of ZnS were carried out at various temperatures viz. 800, 850, 900, 950 and 1000°C. The results of these studies are listed in Tables I to V and are also plotted graphically in Fig. 13. The progress of the oxidation reaction is represented in terms of fractional oxidation. It has been also observed that during the initial period the interface temperature of the pellet was higher than its surroundings. This is shown in Fig. 14. However, at all temperatures, the interface temperature levelled off to the temperature of the surroundings after about 3 to 4 minutes and remained constant during the subsequent oxidation period lasting about one hour.

The effect of air flow rate on the oxidation behaviour of ZnS pellet is illustrated in Fig. 15, which clearly indicates that the oxidation behaviour is unaffected by increasing the flow rate above 500 cc per minute. The effect of particle size range and porosity of the pellet on the oxidation kinetics are shown in Figs. 16 and 17 respectively and the results are tabulated in Table VI.

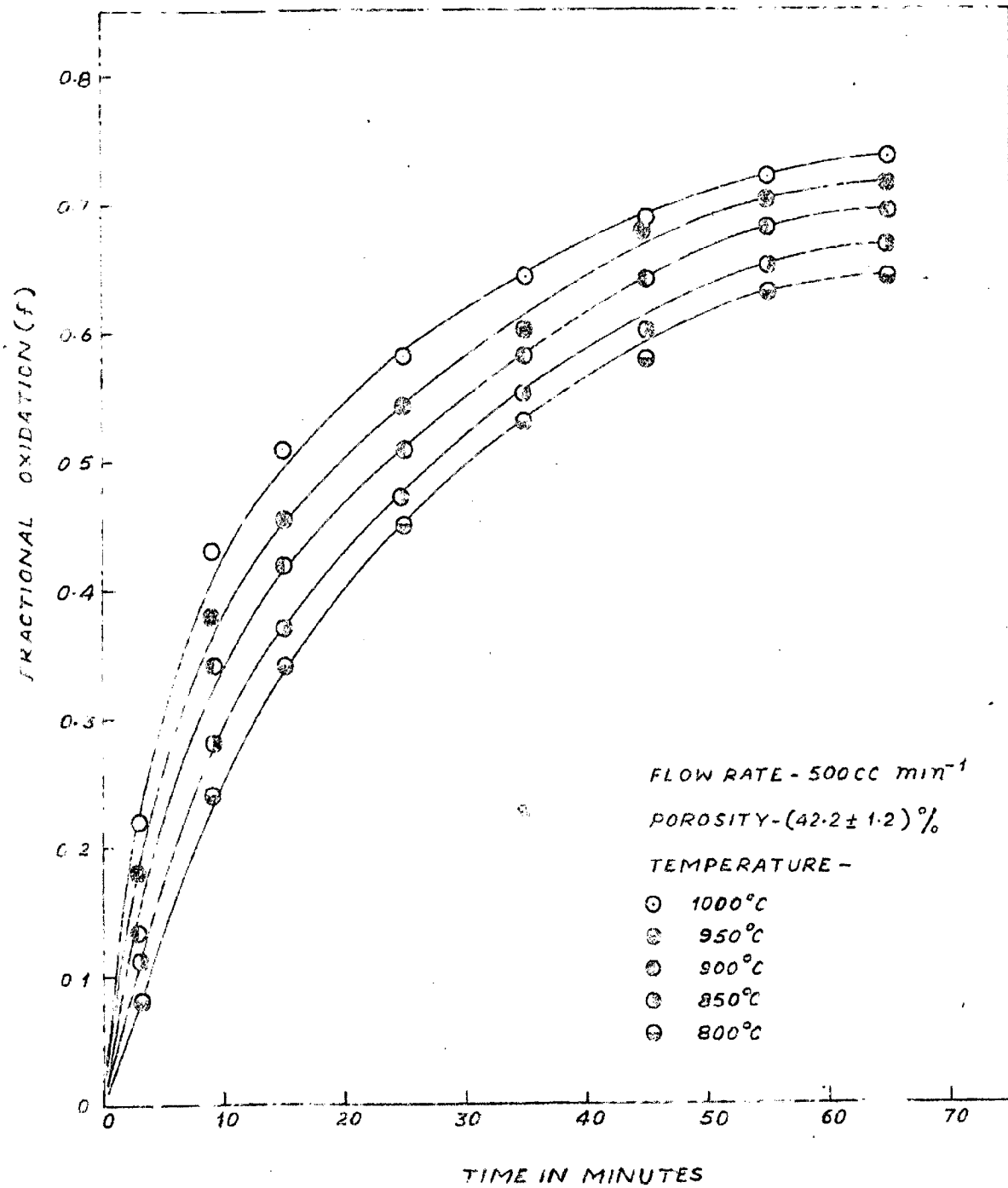


FIG. 13 PLOT OF FRACTIONAL OXIDATION VS TIME FOR ZINC SULPHIDE PELLETS AT VARIOUS TEMPERATURES.

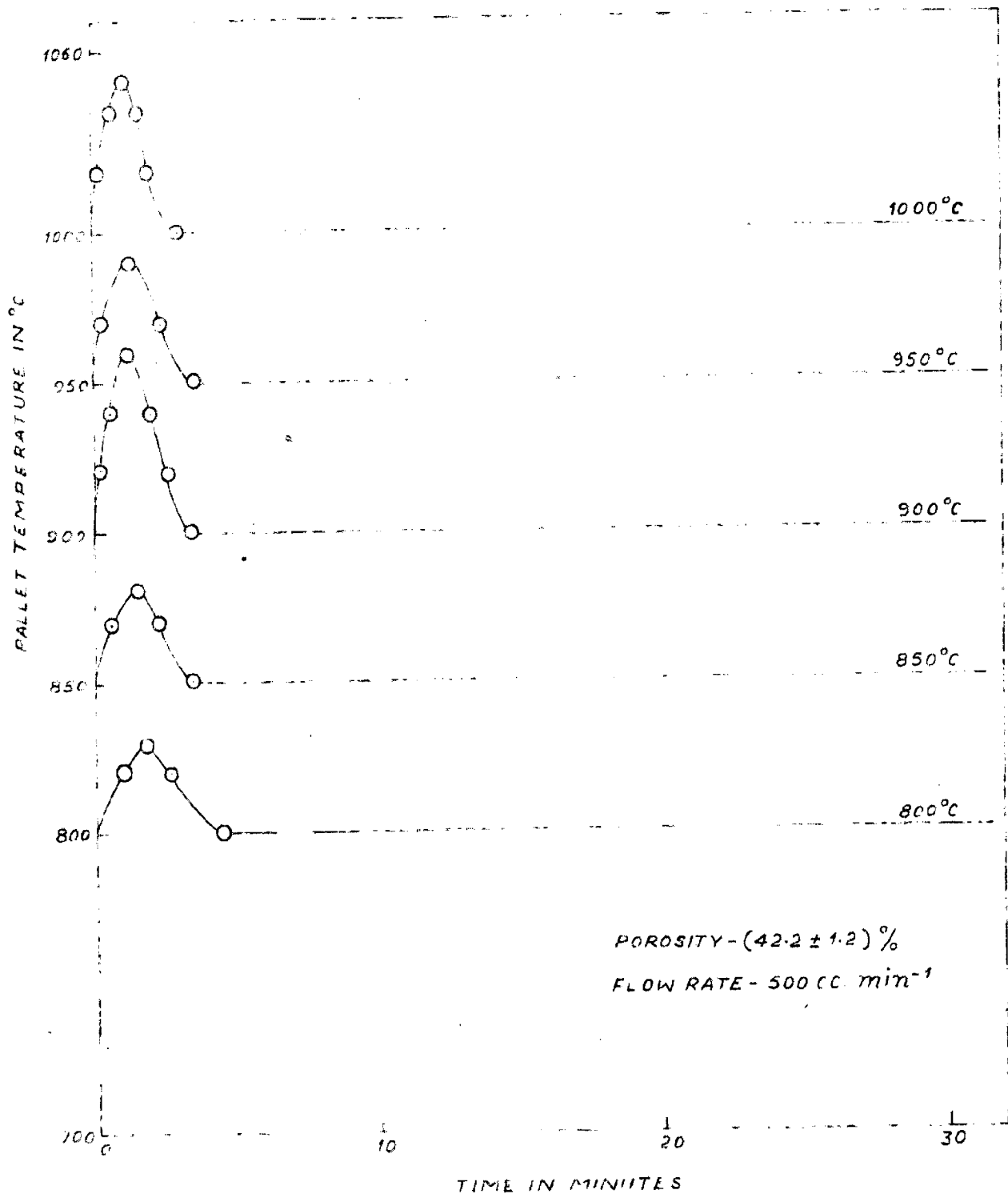


FIG. 10. PLOT OF PELLET TEMPERATURE VS TIME DURING ROASTING OF ZINC SULPHIDE PALLETS.

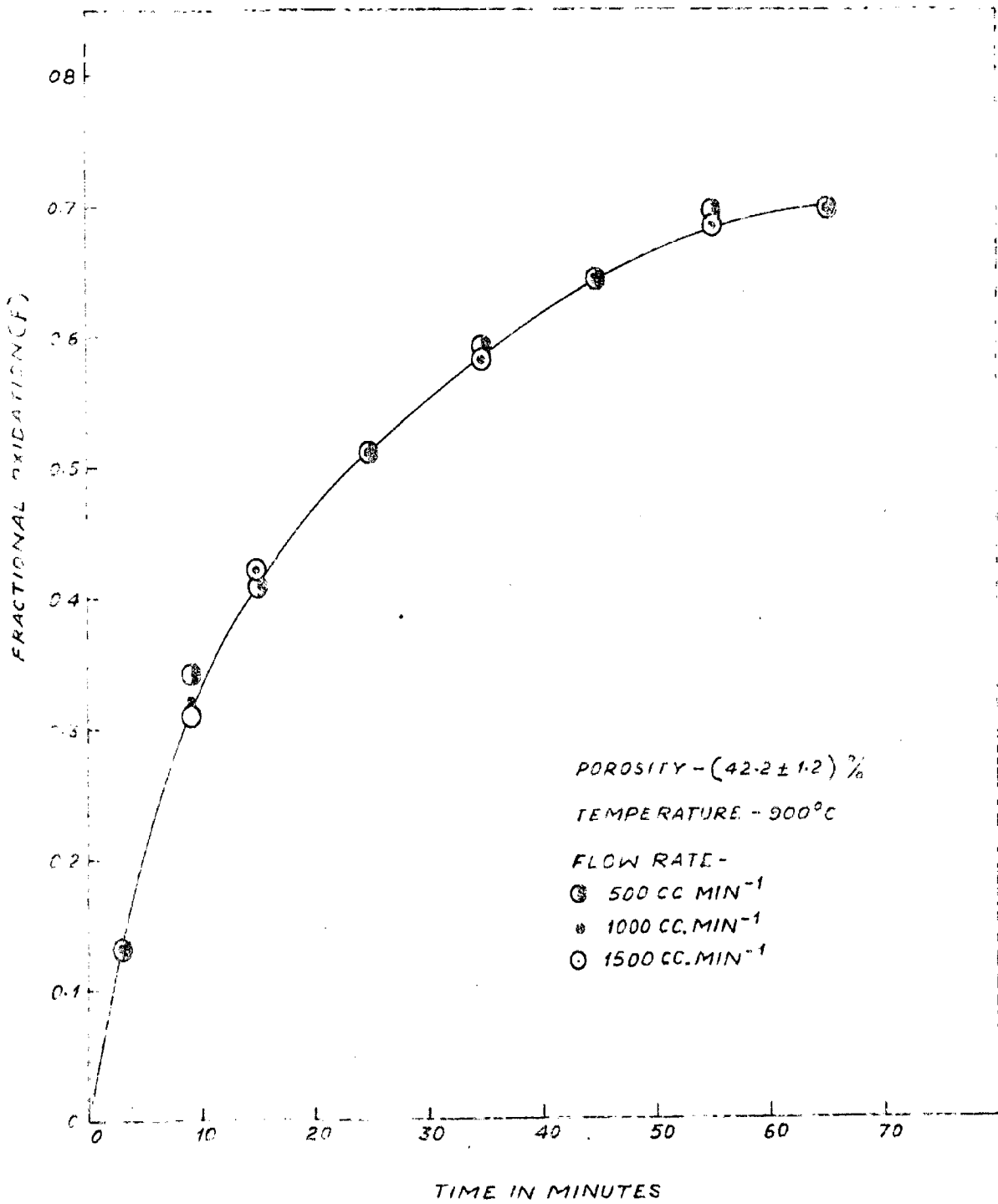


FIG. 13. PLOT OF FRACTIONAL OXIDATION VS TIME FOR ZINC SULPHIDE PELLETS AT DIFFERENT FLOW RATES.

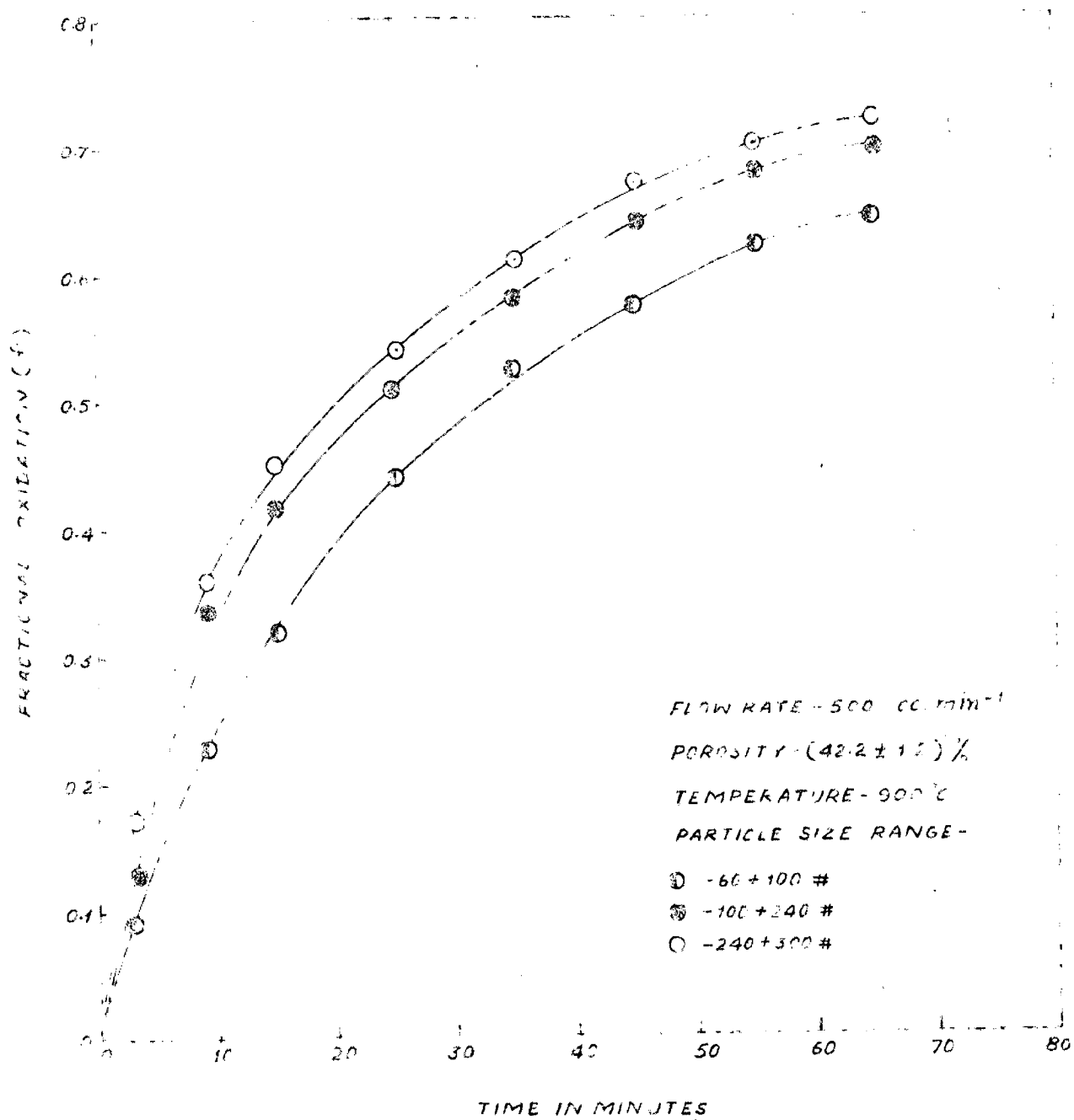


FIG. 10 PLOT OF FRACTIONAL OXIDATION VS TIME FOR ZINC SULPHIDE PELLETS AT DIFFERENT PARTICLE SIZE RANGE



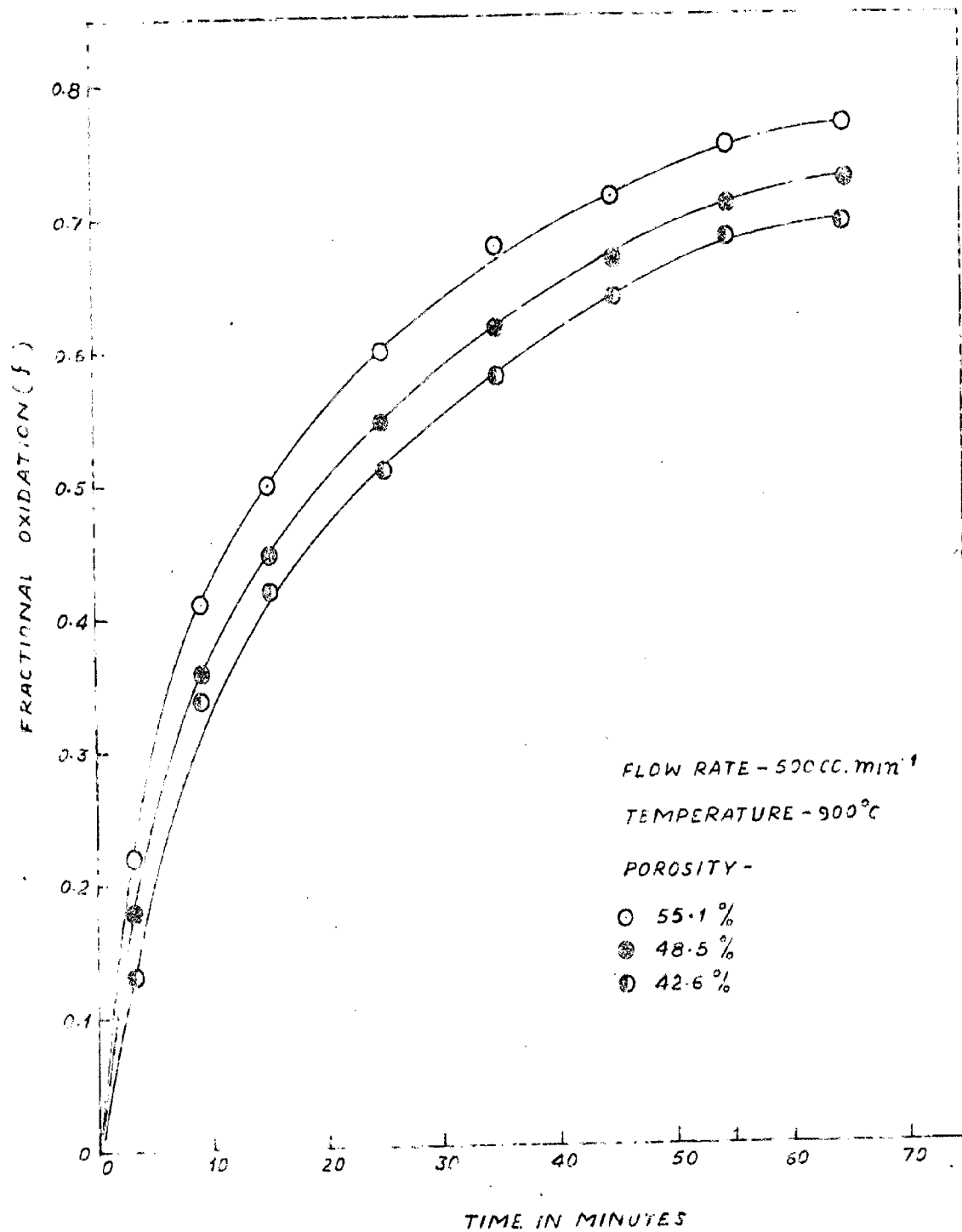


FIG. 17 PLOT OF FRACTIONAL OXIDATION VS TIME FOR ZINC SULPHIDE PELLETS AT VARIOUS POROSITIES.

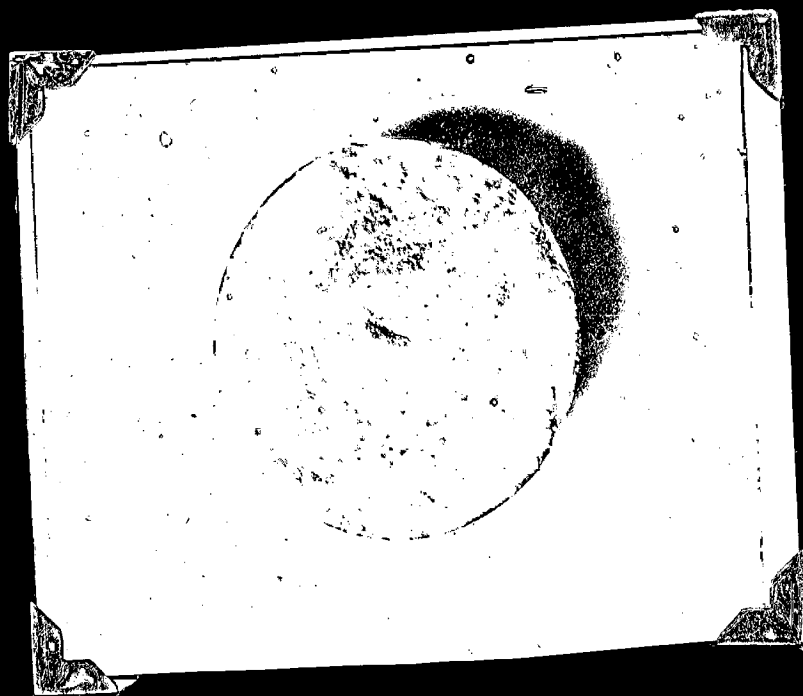


Fig.18. PHOTOGRAPH OF PARTIALLY OXIDIZED PELLET  
OF ZINC SULPHIDE.

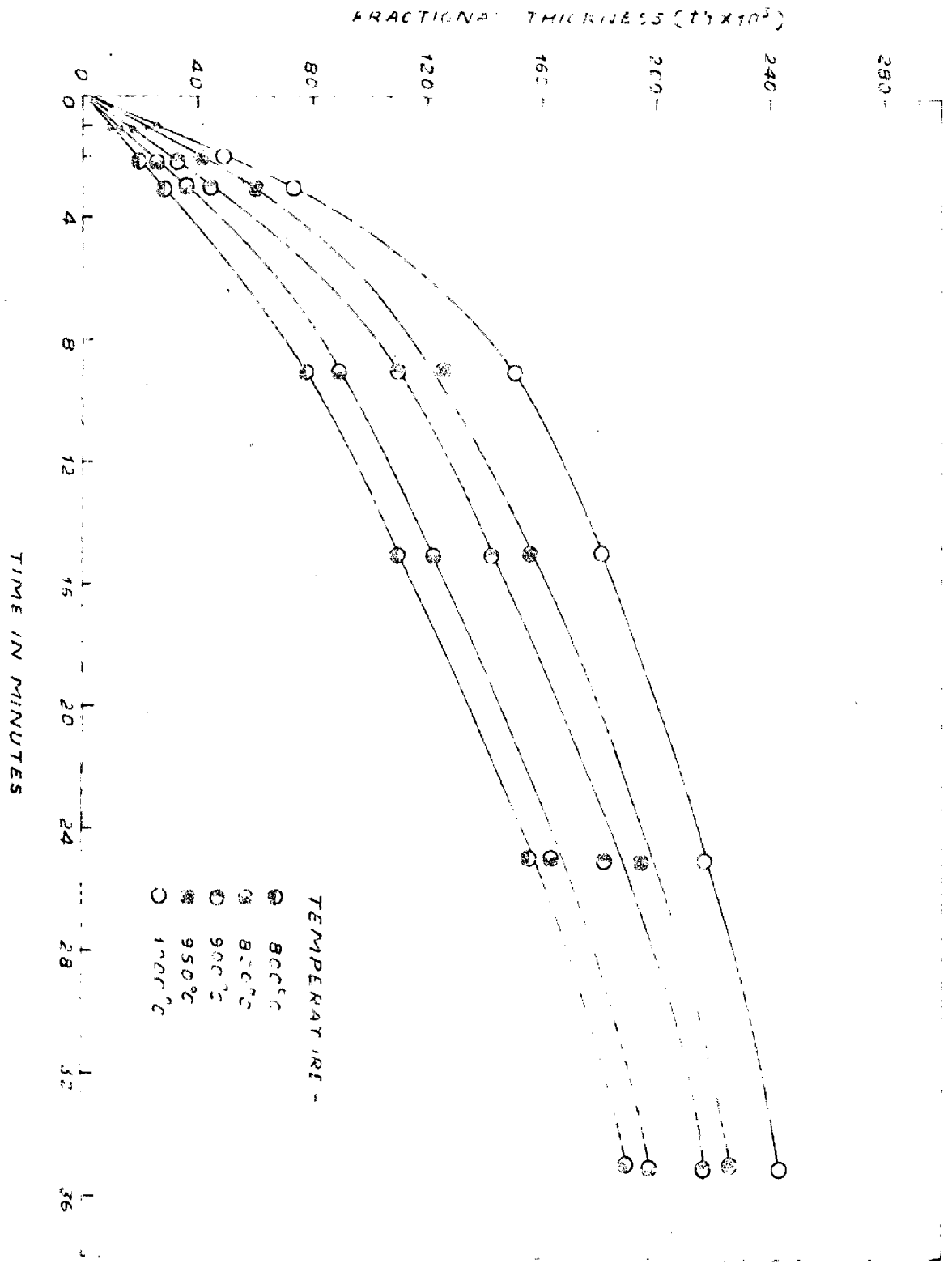


FIG. 20 PLOT OF FRACTIONAL THICKNESS VS TIME FOR ZINC SULPHIDE PELLETS AT VARIOUS TEMPERATURES.

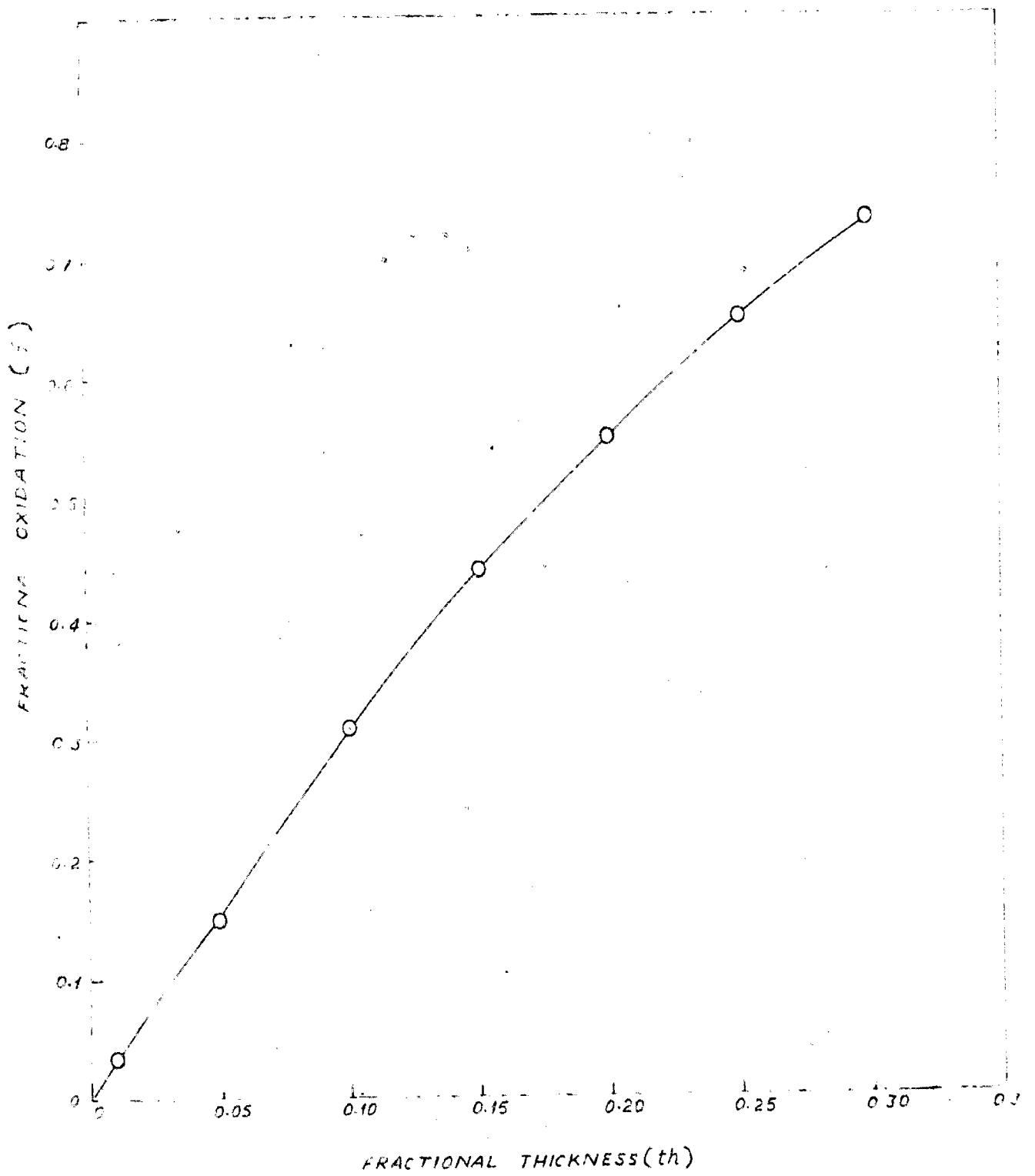


FIG. 19. THEORETICAL PLOT OF FRACTIONAL OXIDATION VS FRACTIONAL THICKNESS FOR ZINC SULPHIDE PELLETS OF DIA. 1.55 CM. AND HEIGHT 1.04 CM.

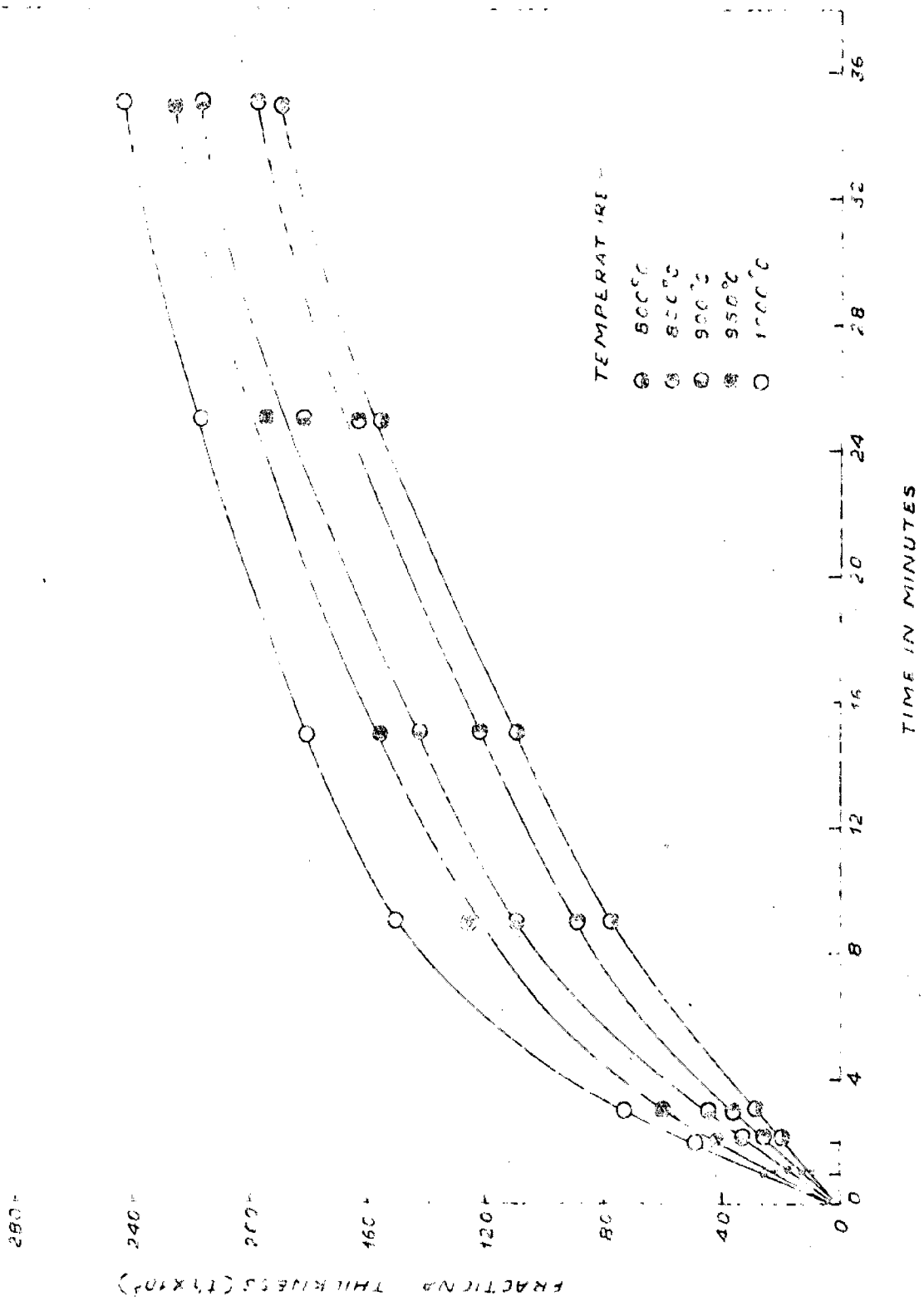


FIG. 20 PLOT OF FRACTIONAL THICKNESS VS TIME FOR ZINC SULPHIDE PELLETS AT VARIOUS TEMPERATURES.

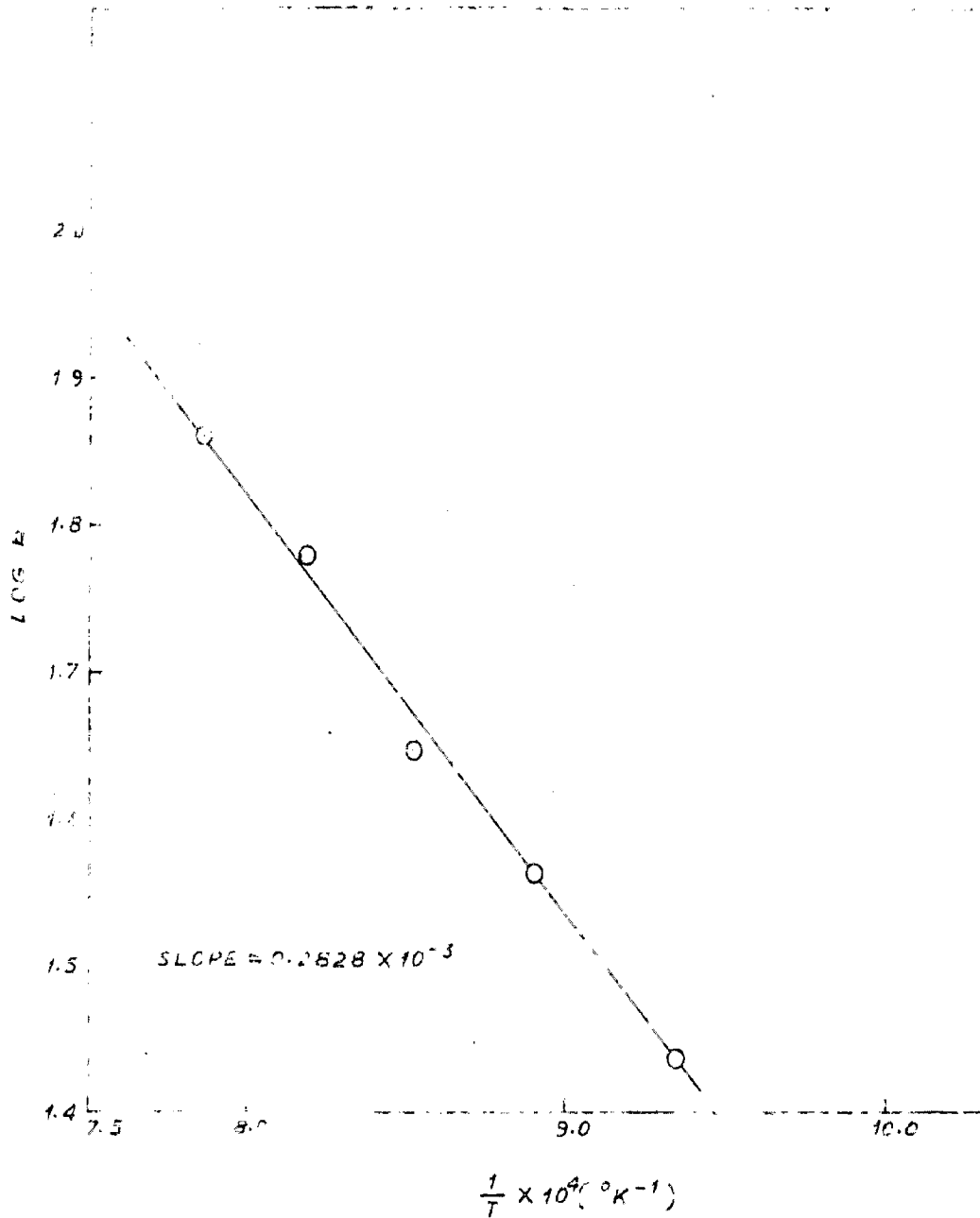


FIG. 21. PLOT OF LOG K VS  $\frac{1}{T}$  FOR THE INITIAL STAGES OF ROASTING OF SULPHIDE PALLETS.

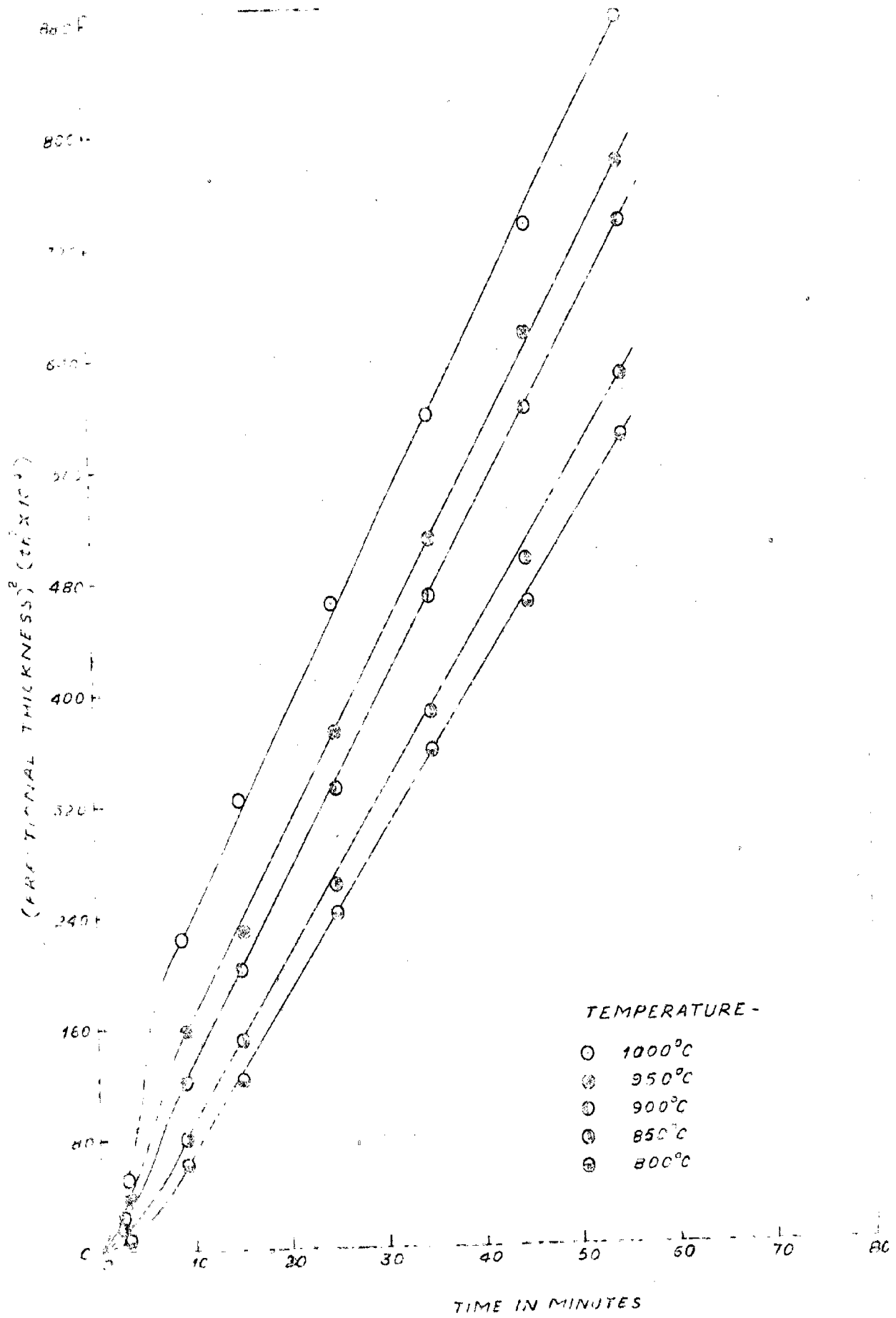


FIG. 22 PLOT OF SQUARE OF FRACTIONAL THICKNESS VS TIME FOR ZINC SULPHIDE PELLETS AT VARIOUS TEMPERATURES.

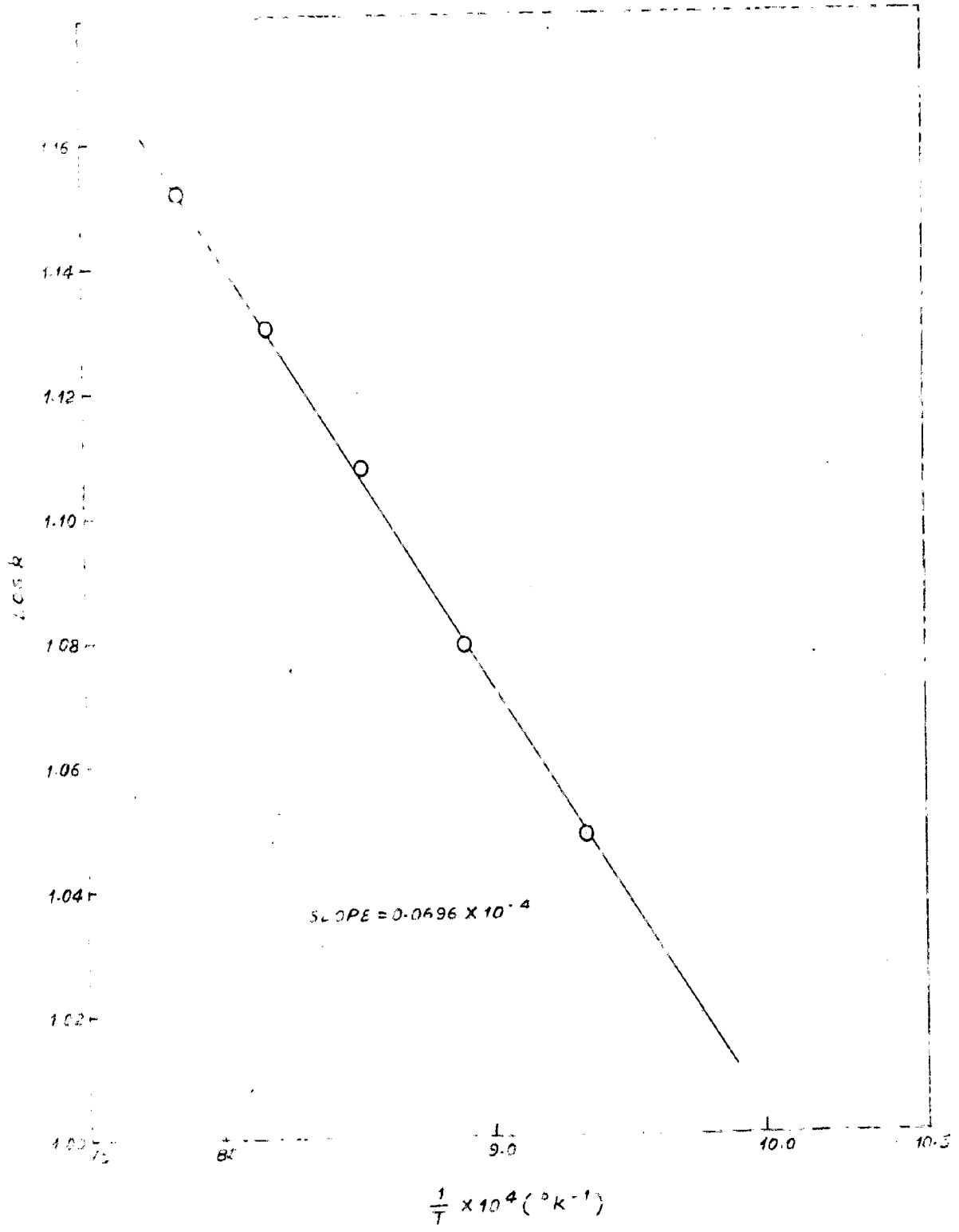


FIG. 23. PLOT OF  $\log R$  VS  $\frac{1}{T}$  FOR LATER STAGE OF ROASTING OF ZINC SULPHIDE PELLETS.



Sectioning of the partially roasted samples confirmed that, in the temperature range of interest, the reaction was always topochemical in nature. A photograph of a partially oxidized pellet of ZnS after sectioning is shown in Fig. 18.

A theoretical curve between fractional oxidation and fractional thickness for a pellet of 1.55 cm diameter and 1.04 cm height is plotted by using the following equation and is shown in Fig. 19., to determine fractional thickness at various experimental values of fractional oxidation.

$$f = 1 - (1 - th)^2 \left( \frac{a - th}{a} \right) \quad (1x)$$

Now these values of fractional thickness and its square are plotted against time and are shown in Figs. 20 and 22 respectively.

The specific reaction rate constants values are then calculated with the help of plots shown in Fig. 20 and 22. The log of specific reaction rate constants are plotted against the reciprocal of the absolute temperature which are shown in Figs. 21 and 23 respectively. The values of activation energies found for the initial and subsequent periods of roasting are  $3.17 \overset{12.91}{\wedge}$  KCal/g. mole and  $12.91 \overset{3.17}{\wedge}$  KCal/g. mole respectively.

#### 4.2 DISCUSSIONS

The experimental data are first analysed to determine the mechanism of the oxidation reaction and

then the effect of various variables on the kinetics of oxidation of zinc sulphide are explained on the basis of zinc sulphide are explained on the basis of the mechanism involved in the reaction.

#### 4.2.1 Mechanism of Roasting

The possible rate controlling steps in the oxidation of ZnS pellet in a stream of dry air may be grouped as,

- (a) Gaseous film resistance
- (b) Shell layer resistance and
- (c) Interface resistance.

Gaseous film resistance is not the rate controlling step as the oxidation rate has become virtually independent of air flow rate after it exceeds 500 cc per minute as shown in Fig. 15. Therefore it appears that in the initial period when the product layer is not sufficiently thick, the reaction at the interface is likely to be the rate controlling step, to be followed by the diffusion controlled process as the ZnO layer is built up. In addition, heat transfer effects have to be taken into consideration while deciding the rate controlling step during the initial period as the pellet temperature increases during the initial stage of roasting.

First, chemical reaction at the interface is assumed to be the rate controlling step. Thus the plot of  $\left[1 - (1-f)^{1/3}\right]$  versus time should give a straight line. This is true in case of a spherical or cylindrical pellets with height to diameter ratio unity. In case of different<sup>(31)</sup> cylindrical geometries, a plot of fractional thickness 'th' versus time should give a straight line.

A graph between fractional oxidation and fractional thickness is plotted assigning different values of 'th' in the above equation and calculating corresponding values of 'f'. These values are tabulated in Table VII. and are plotted in Fig. 19. Now a plot between fractional thickness and time is drawn and is shown in Fig. 20. It gives straight line for the initial period of about 3 minutes which is positive indication of the chemical reaction control mechanism.

By measuring the slopes of these lines in Fig. 20, specific reaction rate constant 'k' values are calculated and are shown in Table VIII. Values of log 'k' are then plotted against reciprocal of absolute temperature and is shown in Fig. 21. Value of activation energy is determined from the slope of line of Fig. 21, which comes out to be 12.91 KCal/g.mole. This value of activation energy is not

the suggestive of a chemical control mechanism as it is too small.

Further, the interface temperature of the pellet has been found to be more than that of surroundings, effect of heat transfer, during the initial period, on the mechanism of the oxidation should be considered. For this, theoretical reaction rates during the initial period based on the concept of mass transfer and heat<sup>(24)</sup> and mass transfer are calculated with the help of equations (x) and (xi) respectively and compared with the experimentally observed values of oxidation rates. The calculations involved in determining the theoretical rates are tabulated in Table IX and the rates comparison is shown in Table X.

The two equations developed by Hills<sup>(24)</sup> used for calculating theoretical rates, are given below,

$$\eta_M = \frac{[p_{O_2}]_G}{\frac{RQ_G}{2\pi(2a+1)(D_{eff})r_0} \left[ \left( \frac{1}{r^*} - 1 \right) + \frac{[D_{eff}]}{\alpha r_0} \right]}$$

(x)

and

$$\eta_{H-M} = \frac{[p_{O_2}]_G}{\frac{RQ_G}{2\pi(2a+1)r_0} \left[ \left( \frac{1}{r^*} - 1 \right) + \frac{1}{\Lambda r_0} \right]}$$

It is obvious from Table X that theoretical reaction rates based on mass transfer concept are always higher than the corresponding experimentally observed rates at all temperatures. While there is a satisfactory agreement between rate values calculated on the concept of heat and mass transfer and experimentally observed values. Thus it may be concluded that during the initial period of oxidation, heat and mass transfer is the rate controlling step.

For the subsequent period of oxidation shell layer resistance is assumed to be the rate controlling step. Chemical reaction control cannot be operative during this period as the plot between fractional thickness and time is no more linear. To ascertain the rate controlling step, Jander's<sup>(32)</sup> diffusion model is applied to the experimental data. This model assumes unidirectional bulk diffusion and that the increase in the thickness of product layer follows the parabolic rate law.

Now a graph between square of the fractional thickness and time is plotted which gives straight line during the subsequent period only and non-linearity is observed during the initial period as shown in Fig. 22. By measuring slope of the lines of Fig. 22, specific reaction rate constant ( $k$ ) values are calculated and are shown in Table xi. The values of  $\log k$  are then plotted against reciprocal of the absolute temperature (Fig. 23)

By measuring the slope of this line value of activation energy is determined and comes out to be 3.17 KCal/g.mole. The linearity of the plot between  $(th)^2$  and time and small value of activation energy can be taken as positive indication for the diffusion controlled mechanism during the subsequent period.

Thus it may now be concluded that diffusive steps are rate controlling throughout the oxidation.

#### 4.2.2. Effect of Variables on the Kinetics of Roasting

On the basis of prevailing mechanism during oxidation period, results of various variables on the oxidation kinetics are explained below :

(e) Effect of Temperature - The effect of temperature and time on the oxidation kinetics is self evident from Fig. 13. In general at all temperatures the reaction is rapid in the initial stages and slows down considerably in later stages. It is explained as due to the increased diffusional resistance as a result of the progressively increase in the thickness of product layer. The increase in the rate of oxidation with the increase in temperature happens because of increased diffusivities and mass transfer coefficients.

The release of exothermic heat is indicated by the rise in the interface temperature from that of surroundings. This exothermic heat also...

controlling the rate of oxidation during the initial period of oxidation.

(b) Effect of Air Flow Rate - To study the effect of air flow rate on the kinetics of oxidation, the air was passed at 500, 1000 and 1500 cc per minute. The results are shown in Fig. 15. It has been found that increased flow rate beyond 500 cc per minute has no effect on the oxidation kinetics of ZnS. It is an indicative of the absence of gas starvation and that the plateau is reached before the air flow rate reaches 500 cc per minute.

(c) Effect of Porosity and Particle Size - Other factors remaining constant, rate of oxidation increases with increase in porosity and decrease in particle size. Increased porosity facilitates diffusion so that faster diffusion of air takes place and rate increases. Smaller particles offers more surface area for the reaction thereby increasing the oxidation rate.

In the present investigation, the porosity of the pellets were 42.6%, 48.5% and 55.1% and size ranges of particles were  $-60 + 100 \mu$ ,  $-100 + 240 \mu$  and  $-240 + 300 \mu$ .

CONCLUSIONS



## CONCLUSIONS

On the basis of results and discussions, following conclusions can be drawn.

- (1) There is rise in the temperature of zinc sulphide sample in the initial period due to conversion of zinc sulphide to zinc oxide. The temperature difference between sample and surroundings is levelled off in the initial 3 to 4 minutes and remains constant during the rest of the period lasting about one hour.
- (2) The values of activation energies are found to be 12.91 and 3.17 KCal/g.mole in the initial and final stages of oxidation respectively. These values suggest that the oxidation process is diffusion controlled.
- (3) The effect of heat and mass transfer on the overall rate is significant at the beginning of the oxidation process when the product layer thickness is small.
- (4) Increasing flow rate increases the rate of oxidation upto 500 cc per minute and beyond this oxidation rate is independent of air flow rate.
- (5) The increased porosity increases the oxidation rate of zinc sulphide sample.
- (6) The decreased size of the particles of zinc sulphide increases the oxidation rate.

## REFERENCES

1. Newton, J., "Extractive Metallurgy", John Wiley & Sons, Inc., New York, 1959, p. 286.
2. Laist, F., Caples, R.B. and Wever, G.T., "Handbook of Non-Ferrous Metallurgy", Liddell, D.M. (Ed.), McGraw Hill Book Company, Inc., New York, 1945, p. 379.
3. Perretti, E.A., Discussions Farad. Soc., 4, 1948, p.174.
4. Denbigh, K.G., and Beveridge, G.S.G., Trans. Inst. Chem. Eng., 40, 1962, p.23.
5. Natesan, K. and Philbrook, W.O., TMS-AIME, 245, 1969, p.2243.
6. Ong, J.N.Jr., Wadsworth, M.E. and Fassell, W.M. Jr, J. Metals, 206, 1956. p.257.
7. Cannon, K.J. and Denbigh, K.G., Chem.Eng.Sci.,6, 1957, p.155.
8. Rao, M.M. and Abraham, K.P., Indian J. Tech., 3, 1965, p.291.
9. Blakemore, W.B., "Solid State Physics", Saunders Company Philadelphia, 1972, p.42.
10. Kittel, C., "Introduction to Solid State Physics", John Wiley & Sons, Inc., New York, 1971, p30.
11. Swalin, R.A., "Thermodynamics of Solids", John Wiley & sons., Inc., New York, 1967, p306.
12. Kurian, E.M. and Tambankar, R.V., Trans. IIM, 23, 1970, p.59.
13. Dimitov, R. and Paulip, A., Rudarko, Met.Zbornik, 3 1965, p.305.

107444

14. Tidwell, L.G. and Larson, A.H., TMS-AIME, 236  
1966, p1379.
16. Ingrahm, T.R. and Kellogg, H.H., Trans. AIME, 227  
1964, p.1419.
16. McCabe, C.L., Trans. AIME, 200 , 1954, p 969
17. Bryukvin, V.A., Burovoi, I.A. and Tsvetkov, Yu, V.,  
Izv. Akad.Nauk.SSR Metally, 3, 1966, p55.
18. Natesan, K. and Philbrook, W.O., TMS-AIME- , 245,  
1969, p.1417.
19. Wadsworth, M.E. and Fassell, W.M. Jr., Trans. AIME,  
197, 1953, p.1556
20. Gilchrist, J.D., Extractive Metallurgy, Pergamon  
Press, Oxford, 1967, p.169.
21. Lu, W.K., Trans. AIME, 227 , 1963, p 203,
22. Lu, W.K. and Betaslanes, G., TMS-AIME, 236, 1966,  
p.531.
23. Jost, W., Chem.Eng. Sci., 2 , 1953, p.199.
24. Hills, A.W.D., "Heat and Mass Transfer in Process  
Metallurgy", Inst. of Min & Met. London, 1967, p.54.
25. Gerlach, J. and Stichel, W., Z.Erzbergbau, Metallhuet-  
tenw, 17 , 1964, p427.
26. Lund, R.E. , Warners, D.E. and Morgan, J.A., Trans.  
AIME, 224, 1962, p 834.
27. Mikhin, Ya, Ya. and Roy, S., Trans.IIM, 18 , 1965,  
p. 148.

28. Roggero, C.E., Trans. AIME, 227, 1963, p105.
29. Rao, M.M. and Abraham, K.P., Indian J. Tech., 4, 1966, p 59.
30. Schwab, G.M. and Philins, J.,J. Am.Chem.Soc., 69 , 1947, p.2588.
31. McKewan, W.M., "The Chipman Conference", Elliot, J.F. (Ed.), The MIT, Press Massachusetts, 1962, p 141.
32. Jander, W., I.Z. Anorg.Chem., 163, 1927, pl.

**APPENDIX**

TABLE - I  
EXPERIMENTAL RESULTS OF ROASTING OF ZnS

Temperature 800°C                      Flow rate 500 cc min<sup>-1</sup>  
Porosity (42.2 ± 1.2)%      Weight of sample 4.6496

Sl. No.	Time (minutes)	Weight loss (gm)	Fractional oxidation (f)	Fractional thickness (th)	(th) <sup>2</sup>
1	1*	0.0191	0.025	0.008	0.000000
2	2	0.0400	0.050	0.016	0.000262
3	3	0.0613	0.081	0.026	0.00068
4	9	0.1840	0.243	0.078	0.00610
5	15	0.2582	0.340	0.110	0.01210
6	25	0.3423	0.451	0.155	0.02400
7	35	0.4011	0.529	0.189	0.03560
8	45	0.4392	0.580	0.214	0.04606
9	55	0.4814	0.634	0.242	0.05814
10	65	0.4885	0.648	0.250	0.06250

\* Calculated from Fig. 13.

TABLE II  
EXPERIMENTAL RESULTS OF ROASTING OF ZnS

Temperature 850°C                      Flow rate 500 cc min<sup>-1</sup>  
Porosity (4.22 ± 1.2)%                  Weight of sample 4.6852 gm

S No.	Time (min.)	Weight loss (gm)	Fractional oxidation (f)	Fractional thickness (th)	(th) <sup>2</sup>
1	1*	0.0273	0.035	0.012	0.00014
2	2	0.0547	0.070	0.024	0.00058
3	3	0.0855	0.112	0.036	0.00131
4	9	0.2152	0.281	0.091	0.00811
5	15	0.2852	0.374	0.122	0.01484
6	25	0.3434	0.449	0.155	0.02405
7	35	0.4125	0.540	0.196	0.03846
8	45	0.4591	0.601	0.222	0.04904
9	55	0.4972	0.650	0.250	0.06250
10	65	0.5133	0.671	0.262	0.07014

\* Calculated from Fig. 13.

TABLE III

EXPERIMENTAL RESULTS OF ROASTING OF ZnS

Temperature  $900^{\circ}\text{C}$  Flow rate  $500\text{ cc min}^{-1}$   
 Porosity  $(42.2 \pm 1.2)\%$  Weight of sample  $4.6627\text{ gm}$

S No.	Time (minutes)	Weight loss (gm)	Fractional oxidation (f)	Fractional thickness (th)	$(\text{th})^2$
1	1*	0.0306	0.04	0.014	0.00020
2	2	0.0686	0.09	0.030	0.00090
3	3	0.0995	0.131	0.044	0.00196
4	9	0.2600	0.342	0.111	0.01211
5	15	0.3193	0.420	0.142	0.02004
6	25	0.3811	0.513	0.182	0.03276
7	35	0.4422	0.581	0.216	0.04656
8	45	0.4481	0.643	0.246	0.06016
9	55	0.5183	0.681	0.270	0.07290
10	65	0.5291	0.695	0.277	0.07319

\* Calculated from Fig. 13



TABLE IV

EXPERIMENTAL RESULTS OF ROASTING OF ZnS

Temperature 950°C                      Flow rate 500 cc min<sup>-1</sup>  
 Porosity (42.2 ± 1.2) %                  Weight of sample 4.6128 gm

S. No.	Time (minutes)	weight	Fractional	Fractional	(th) <sup>2</sup>
		loss (gm)	oxidation (f)	thickness (th)	
1	1*	0.0452	0.060	0.020	0.00040
2	2	0.904	0.120	0.040	0.00160
3	3	0.1361	0.181	0.60	0.00360
4	9	0.2882	0.383	0.126	0.01586
5	15	0.3234	0.430	0.150	0.02250
6	25	0.4110	0.544	0.194	0.03746
7	35	0.4521	0.600	0.225	0.05045
8	45	0.5414	0.671	0.262	0.06804
9	55	0.5280	0.701	0.281	0.07801
10	65	0.5382	0.715	0.288	0.08304

\* Calculated from Fig. 13.

TABLE V

EXPERIMENTAL RESULTS OF ROASTING OF ZnS

Temperature 1000°C                      Flow rate 50 cc min<sup>-1</sup>  
 Porosity (42.2 ± 1.2)%                      Weight of sample 4.5989 gm

S. No.	Time (minute)	weight loss (gm)	Fractional oxidation 'f'	Fractional thickness 'th'	(th) <sup>2</sup>
1	1*	0.0525	0.070	0.024	0.00058
2	2	1.0499	0.140	0.047	0.00230
3	3	0.1655	0.221	0.0725	0.00518
4	9	0.3221	0.430	0.150	0.02250
5	15	0.3836	0.512	0.182	0.03244
6	25	0.4372	0.583	0.216	0.04646
7	35	0.4810	0.641	0.242	0.05954
8	45	0.5092	0.680	0.268	0.07204
9	55	0.5413	0.723	0.296	0.08816
10	65	0.5506	0.735	0.304	0.09242

\* Calculated from Fig. 13

TABLE VI

## EXPERIMENTAL RESULTS OF ROASTING OF ZnS

Temperature 900°C ✓

S. No.	Flow rate (cc. min <sup>-1</sup> )	Porosity (%)	Particle size ( $\mu$ )	Initial weight of sample (gm)	Time (minutes)	Weight loss (gm)	Fractional oxidation (f)
1	2	3	4	5	6	7	8
1	500	42.6	-100+ 240	4.6124	3	0.1015	0.135
					9	0.3006	0.379
					15	0.3162	0.420
					25	0.3854	0.512
					35	0.4383	0.583
					45	0.4811	0.639
					55	0.5124	0.681
	65	0.5221	0.694				
-----							
2	500	48.5	-100 +240	4.2734	3	0.1261	0.181
					9	0.2525	0.362
					15	0.3483	0.449
					25	0.3802	0.545
					35	0.4292	0.616
					45	0.4654	0.667
					55	0.4948	0.709
	65	0.5127	0.725				
-----							
3	500	55.1	-100 +240	3.5826	3	0.1241	0.212
					9	0.2407	0.410
					15	0.2936	0.502
					25	0.3517	0.600
					35	0.3971	0.678
					45	0.4211	0.717
					55	0.4392	0.751
	65	0.4489	0.766				
-----							
4	1600	42.2 +1.2	-100 +240	4.6328	3	0.0991	0.132
					9	0.2413	0.318
					15	0.3174	0.420
					25	0.3861	0.511
					35	0.4416	0.582
					45	0.4731	0.626
					55	0.5164	0.683
	65	0.5259	0.695				

Table VI (Contd..)

1	2	3	4	5	6	7	8
					3	0.0988	0.131
					9	0.2357	0.312
					15	0.3132	0.415
5	1500	42.2	-100	4.6284	25	0.3848	0.510
		+1.2	+240		35	0.4441	0.589
					45	0.4831	0.641
					55	0.5193	0.688
					65	0.5243	0.695
-----							
					3	0.712	0.994
					9	0.1731	0.229
					15	0.2423	0.320
6	500	42.2	-60	4.6421	25	0.3331	0.441
		+1.2	+100		35	0.3974	0.526
					45	0.4343	0.574
					55	0.4692	0.621
					65	0.4869	0.643
-----							
					3	0.1291	0.171
					9	0.5732	0.362
					15	0.3396	0.450
7	500	42.2	-240	4.6411	25	0.4106	0.543
		+1.2	+300		35	0.4619	0.611
					45	0.5086	0.673
					55	0.5263	0.698
					65	0.5412	0.718

TABLE VII

VALUES OF FRACTIONAL THICKNESS AND FRACTIONAL  
OXIDATION FOR ROASTING OF ZnS PELLET WITH 'a'  
EQUAL TO 0.672

S. No.	Fractional thickness (th)	Fractional oxidation 'f'
1	0.01	0.035
2	0.05	0.148
3	0.10	0.310
4	0.15	0.440
5	0.20	0.552
6	0.25	0.648
7	0.30	0.731

TABLE VIII

SPECIFIC REACTION RATE CONSTANT (k) VALUES AT DIFFERENT  
TEMPERATURES FOR ROASTING OF ZnS

S. No.	Temperature 'T' °K	$\frac{1}{T} \times 10^4$ (°K <sup>-1</sup> )	Specific reaction rate constant (k) $k \times 18 \times 10^4$	log k
1	1073	9.34	26.0	1.4345
2	1123	8.90	36.0	1.5563
3	1173	8.52	44.0	1.6435
4	1223	8.16	60.0	1.7782
5	1273	7.86	72.0	1.8573

TABLE IX  
CALCULATIONS INVOLVED IN THE DETERMINATION OF THEORETICAL RATES OF  
ROASTING OF ZnS

Diameter of the furnace tube ( $D_T$ ) = 5 cm.

Air flow rate = 500 cc min<sup>-1</sup>, Porosity = (42.2 + 1.2) %

Diameter of the pellet (d) = 1.550 cm, Value of a = 0.672

$\epsilon = 0.60$ ,  $\gamma = 0.514$ ,  $T = 01.5$

Parameter	Its value at different temperature				
	800	850°C	900°C	950°C	1000°C
$\rho_a$	$1.15 \times 10^{-3}$	$1.10 \times 10^{-3}$	$1.08 \times 10^{-3}$	$1.07 \times 10^{-3}$	$1.05 \times 10^{-3}$
$\mu \times 10^4$	4.2	4.3	4.4	4.6	4.7
D	0.75	0.83	0.91	1.01	1.11
Re	1.79	1.68	1.63	1.50	1.46
$S_c$	0.510	0.475	0.470	0.465	0.455
$K \times 10^4$	1.64	1.72	1.79	1.87	1.95
$h_{conv} \times 10^4$	2.98	3.10	3.22	3.32	3.42
$h_{rad} \times 10^3$	4.00	4.60	5.35	5.96	6.73
$h_{tot} \times 10^3$	4.298	4.910	5.672	6.292	7.072
$K_s \times 10^4$	13.60	13.64	13.69	13.73	13.77
$\Delta H \times 10^{-5}$	1.0756	1.0759	1.0771	1.0778	1.0786
Pr	0.695	0.695	0.695	0.695	0.695
$(\frac{1}{R}-1)$ for 1 min	0.0081	0.0142	0.0163	0.0267	0.0308
$\alpha$	1.32	1.44	1.60	1.76	1.95
Deff	0.129	0.144	0.159	0.177	0.194
$\Lambda$	0.286	0.363	0.455	0.588	0.675
$\Gamma$	0.061	0.070	0.078	0.091	0.099

TABLE X  
COMPARISON OF THEORETICAL AND EXPERIMENTALLY OBSERVED  
RATES OF ROASTING OF ZnS

Temp- era- ture °C	S. No.	Theoretical rate of oxidation based on mass transfer concept (g.mole/sec)	Theoretical rate of oxidation based on the concept of heat and mass transfer (g. mole/sec)	Experimentally observed rate of oxidation (g. mole/sec.)
800	1	$2.60 \times 10^{-5}$	$0.59 \times 10^{-5}$	$0.65 \times 10^{-5}$
850	2	$2.64 \times 10^{-5}$	$0.71 \times 10^{-5}$	$0.92 \times 10^{-5}$
900	3	$2.77 \times 10^{-5}$	$0.82 \times 10^{-5}$	$1.04 \times 10^{-5}$
950	4	$2.83 \times 10^{-5}$	$0.93 \times 10^{-5}$	$1.51 \times 10^{-5}$
1000	5	$2.92 \times 10^{-5}$	$1.06 \times 10^{-5}$	$1.80 \times 10^{-5}$

TABLE XI  
PARABOLIC RATE CONSTANT 'k<sub>p</sub>' VALUES AT DIFFERENT TEMPERATURES  
FOR ROASTING OF ZINC SULPHIDE

S. No.	Tempera- ture 'T' °K	$\frac{1}{T} \times 10^4$ (°K <sup>-1</sup> )	Specific reaction rate constant (k <sub>p</sub> × 6 × 10 <sup>5</sup> )	log k <sub>p</sub>
1	1073	9.34	11.20	1.0492
2	1123	8.90	12.00	1.0791
3	1173	8.52	12.80	1.1072
4	1223	8.16	13.50	1.1303
5	1273	7.86	14.20	1.1522